

AD A 139136

12

ADF 300388

MEMORANDUM REPORT ARBRL-MR-03334  
(Supersedes IMR No. 778)

FLIGHT DATA ON LIQUID-FILLED SHELL  
FOR SPIN-UP INSTABILITIES

William P. D'Amico, Jr.

February 1984

RECEIVED  
ELECTRONICS  
MAR 5 1984  
AA



US ARMY ARMAMENT RESEARCH AND DEVELOPMENT CENTER  
**BALLISTIC RESEARCH LABORATORY**  
ABERDEEN PROVING GROUND, MARYLAND

Approved for public release; distribution unlimited.

DTIC FILE COPY

84 03 05 019

Destroy this report when it is no longer needed.  
Do not return it to the originator.

Additional copies of this report may be obtained  
from the National Technical Information Service,  
U. S. Department of Commerce, Springfield, Virginia  
22161.

The findings in this report are not to be construed as  
an official Department of the Army position, unless  
so designated by other authorized documents.

*The use of trade names or manufacturers' names in this report  
does not constitute endorsement of any commercial product.*

UNCLASSIFIED

SECURITY CLASSIFICATION OF THIS PAGE (When Data Entered)

REPORT DOCUMENTATION PAGE		READ INSTRUCTIONS BEFORE COMPLETING FORM
1. REPORT NUMBER MEMORANDUM REPORT ARBRL-MR-03334	2. GOVT ACCESSION NO. ADA 139 136	3. RECIPIENT'S CATALOG NUMBER
4. TITLE (and Subtitle) FLIGHT DATA ON LIQUID-FILLED SHELL FOR SPIN-UP INSTABILITIES	5. TYPE OF REPORT & PERIOD COVERED Final	
	6. PERFORMING ORG. REPORT NUMBER	
7. AUTHOR(s) William P. D'Amico, Jr.	8. CONTRACT OR GRANT NUMBER(s)	
9. PERFORMING ORGANIZATION NAME AND ADDRESS U.S. Army Ballistic Research Laboratory, ARDC ATTN: DRSMC-DLL(A) Aberdeen Proving Ground, Maryland 21005	10. PROGRAM ELEMENT, PROJECT, TASK AREA & WORK UNIT NUMBERS RDT&E 1L162618AH80	
11. CONTROLLING OFFICE NAME AND ADDRESS US Army AMCCOM, ARDC Ballistic Research Laboratory, ATTN:DRSMC-BLA-S(A) Aberdeen Proving Ground, Maryland 21005	12. REPORT DATE February 1984	
	13. NUMBER OF PAGES 52	
14. MONITORING AGENCY NAME & ADDRESS (if different from Controlling Office)	15. SECURITY CLASS. (of this report) Unclassified	
	16. DECLASSIFICATION/DOWNGRADING SCHEDULE	
16. DISTRIBUTION STATEMENT (of this Report) Approved for public release; distribution unlimited.		
17. DISTRIBUTION STATEMENT (of the abstract entered in Block 20, if different from Report)		
18. SUPPLEMENTARY NOTES This report supersedes IMR 778, dated May 1983.		
19. KEY WORDS (Continue on reverse side if necessary and identify by block number) Liquid-Filled Shell Spin-Up Yawsonde		
20. ABSTRACT (Continue on reverse side if necessary and identify by block number) (bja) The stability of a spinning projectile can be adversely affected when a liquid payload is present. Due to the impulsive launch of a spin-stabilized projectile, the liquid payload is subjected to unsteady and time-dependent processes. For example, the liquid must adjust to the rapid spin of the projectile casing. This process is normally called liquid spin-up. For many		

(continued)

UNCLASSIFIED

SECURITY CLASSIFICATION OF THIS PAGE(When Data Entered)

projectiles, the liquid spin-up process encompasses a large portion of the trajectory, and in fact many flight instabilities have occurred during this spin-up time frame. Flight data for spin-up instabilities of 155mm projectiles are presented and qualitatively discussed with respect to a recently developed model for yaw moments during spin-up.

UNCLASSIFIED

SECURITY CLASSIFICATION OF THIS PAGE(When Data Entered)



## LIST OF ILLUSTRATIONS

<u>Figure</u>	<u>Page</u>
1 Spin-Up Eigenfrequency History for an M687L (k = 7, n = 1).....	16
2 Spin-Up Eigenfrequency Histories for an M687A (k = 7, n = 1).....	17
3 Spin-Up Eigenfrequency Histories for an M687B (k = 5, n = 1).....	18
4 Sectioned View of a Standard M687, 155mm, Binary Projectile.....	19
5a Sigma N Versus Time for A1-1.....	20
5b Spin Versus Time for A1-1.....	21
6a Sigma N Versus Time for A1-2 (0-40 Sec).....	22
6b Sigma N Versus Time for A1-2 (0-15 Sec).....	23
6c Spin Versus Time for A1-2.....	24
7a Sigma N Versus Time for A1-3 (0-40 Sec).....	25
7b Sigma N Versus Time for A1-3 (0-15 Sec).....	26
7c Spin Versus Time for A1-3.....	27
8a Sigma N Versus Time for A1-4 (0-40 Sec).....	28
8b Sigma N Versus Time for A1-4 (0-15 Sec).....	29
8c Spin Versus Time for A1-4.....	30
9a Sigma N Versus Time for A50-1 (0-40 Sec).....	31
9b Sigma N Versus Time for A50-1 (0-15 Sec).....	32
9c Spin Versus Time for A50-1.....	33
10a Sigma N Versus Time for B1-1 (0-40 Sec).....	34
10b Sigma N Versus Time for B1-1 (0-15 Sec).....	35
10c Spin Versus Time for B1-1.....	36
11a Sigma N Versus Time for B1-2 (0-40 Sec).....	37
11b Sigma N Versus Time for B1-2 (0-15 Sec).....	38

LIST OF ILLUSTRATIONS

<u>Figure</u>	<u>Page</u>
11c Spin Versus Time for B1-2.....	39
12a Sigma N Versus Time for B1-3 (0-40 Sec).....	40
12b Sigma N Versus Time for B1-3 (0-15 Sec).....	41
12c Spin Versus Time for B1-3.....	42
13a Sigma N Versus Time for B50-1.....	43
13b Spin Versus Time for B50-1.....	44
14a $C_{LSM}$ During Spin-Up for $c/a = 5.20$ .....	45
14b $C_{LSM}$ During Spin-Up for $c/a = 3.12$ .....	46

## I. INTRODUCTION

A spinning liquid can support waves within its interior. These waves have been studied extensively in rotating flows and are commonly known as inertial waves.<sup>1</sup> For a cylinder filled with a viscous liquid that is spinning as a quasi-rigid body, the wave frequencies (the eigenfrequencies) depend upon the cylinder aspect ratio (half height/radius =  $c/a$ ), the liquid fill ratio, and Reynolds number ( $Re$ , defined in subsequent discussions). When a liquid-filled projectile is launched, the payload must be spun up by the projectile. The circumferential velocity of the liquid varies during spin-up, and the values of the liquid eigenfrequencies will also depend upon this time-dependent velocity distribution. When the liquid is spinning as rigid body, the destabilizing liquid moment can be computed by several methods.<sup>2,3,4</sup> All of these models have been correlated against experimental data and are consistent for  $Re > 1,000$ . Detailed information about spin-up is available in two areas: unperturbed velocity histories<sup>5,6,7,8</sup> and eigenvalues of the liquid during spin-up.<sup>9</sup> Recently, however, Murphy has developed an approximate scheme for the determination of yaw moments during spin-up.<sup>10</sup>

1. H. P. Greenspan, The Theory of Rotating Fluids, Cambridge University Press, London and New York, 1968.
2. Charles H. Murphy, "Angular Motion of a Spinning Projectile With a Viscous Liquid Payload," BRL Memorandum Report ARBRL-MR-03194, August 1982 (AD A118676). See also Journal of Guidance, Control, and Dynamics, Vol. 6, July-August 1983, pp. 280-286.
3. Nathan Gerber and Raymond Sedney, "Moment on a Liquid-Filled Spinning and Nutating Projectile: Solid Body Rotation," BRL Technical Report ARBRL-TR-02470, February 1983 (AD A125332).
4. E. H. Wedemeyer, "Viscous Corrections to Stewartson's Stability Criterion," BRL Report No. 1325, June 1966 (AD 489687).
5. E. H. Wedemeyer, "The Unsteady Flow Within a Spinning Cylinder," BRL Report No. 1225, October 1963 (AD 431846). Also Journal of Fluid Mechanics, Vol. 20, Part 3, 1964, pp. 383-399.
6. C. W. Kitchens, Jr., "Ekman Compatibility Conditions in Wedemeyer Spin-Up Model," The Physics of Fluids, Vol. 23, No. 5, May 1980, pp. 1062-1064.
7. C. W. Kitchens, Jr., "Navier-Stokes Solutions for Spin-Up From Rest in a Cylindrical Container," BRL Technical Report ARBRL-TR-02193, September 1979 (AD A077115).
8. Raymond Sedney and Nathan Gerber, "Viscous Effects in the Wedemeyer Model of Spin-Up From Rest," BRL Technical Report ARBRL-TR-02493, June 1983 (AD A129506).
9. R. Sedney and N. Gerber, "Oscillations of a Liquid in a Rotating Cylinder: Part II. Spin-Up," BRL Technical Report TR-02489, May 1983 (AD A129094).
10. Charles H. Murphy, "Moment Induced by Liquid Payload During Spin-Up Without a Critical Layer," BRL Technical Report in preparation.

This report describes the results of a flight test where spin-up instabilities were obtained. The design rationale and flight data are discussed. The design of the test was heuristic in nature since at that time a predictive model for a spin-up liquid moment did not exist. A destabilizing liquid moment can become large when an eigenfrequency ( $\tau_{kn}$ ) is nearly equal to the yaw frequency of the projectile ( $\tau$ ). (The mode numbers  $k$  and  $n$  will be explained in the next section.) The overall stability of the liquid-projectile system, however, depends upon the relative size of the destabilizing liquid moment and the aerodynamic damping moment.

## II. SPIN-UP INSTABILITIES

### A. Spin-up Eigenfrequencies

Assume that a projectile experiences a liquid-induced moment during spin-up. This liquid moment may be short-lived since a change in the circumferential velocity distribution will produce a change in the liquid eigenfrequency. If the total spin-up moment is sufficiently large to induce a growth in yaw, then the growth rate would have the following functional form:

$$\text{Yaw Growth Rate} = F(\tau, \tau_{kn}, d\tau_{kn}/dt) \quad (1)$$

A simple analytic expression for the function  $F$  is not possible. However, it is clear that the yaw growth will be inversely related to  $d\tau_{kn}/dt$ , which is the time variation at the liquid eigenfrequency during spin-up. If  $d\tau_{kn}/dt$  is small the spin-up moment will be large since the resonant behavior will persist for a substantial period of time. On the other hand, if  $d\tau_{kn}/dt$  is large (this is normally the case for early flight times) then the time duration of the moment will be short and the yaw may be only slightly affected. In the design of actual hardware, the physical characteristics of the projectile metal parts specify  $\tau$  and can not be varied to any great degree. However, the yaw growth rate could be controlled through  $d\tau_{kn}/dt$  which is a sensitive function of  $Re$  and  $c/a$ . Using this simple concept, spin-up eigenfrequency histories were computed and canister geometries and liquids were chosen to yield particular values of  $c/a$  and  $Re$ . (Only fill ratios of 100% were used.) Conditions were selected which would produce a resonant matching between a spin-up eigenfrequency and the dimensionless yaw frequency (fast precession frequency/spin frequency). Many combinations of  $Re$  and  $c/a$  were computed. Because the magnitude of the liquid moment was still unknown, a prediction of yaw growth could not be made. Using the method outlined in Reference 9, histograms of spin-up eigenfrequencies were computed. A typical computation is presented in Figure 1 for a 155mm projectile. The solid line is a computed spin-up eigenfrequency history for  $c/a = 4.972$  and  $Re = 1.85 \times 10^6$ . The computational scheme is started at long times where the steady state eigenfrequency is known from any of the linear theories and is advanced backwards in time. At some very early time (normally less than 1 second) the scheme will not converge, but this minor shortcoming did not impact the design of the

experiment (and does not produce any practical difficulties with the general use of this program as an aid to projectile designers).

Spin-up is controlled by the Ekman number ( $E$ ), which is defined as  $v/c\dot{\phi}$  and represents the relative magnitude of the viscous and Coriolis accelerations. In Reference 1 it is shown that the characteristic time to spin-up (the e-folding time) is

$$t(\text{spin-up}) = E^{-1/2} \dot{\phi}^{-1} \quad (2)$$

Historically, in many liquid-filled shell analyses, a Reynolds number ( $Re$ ) is defined as  $a^2\dot{\phi}/\nu$ ; hence,  $Re = (c/a)^2/E$ . Strictly speaking, spin-up flows should be addressed in terms of  $E$ , but  $Re$  will be used for historical consistency. The liquids used in the flight tests were silicone oils of 1 and 50 centistokes (cs) viscosity. Water (under standard conditions) has a kinematic viscosity of approximately 1 cs or  $1 \text{ cm}^2/\text{sec}$ . The densities of the 1 and 50 cs oils are 0.853 and 0.960 gm/cc, respectively.

For simplicity, assume that the spin of the projectile does not decrease from the launch spin rate. Under this condition, the liquid will achieve a state of rigid body rotation at sufficiently long times and the liquid eigenfrequencies can be predicted by the linear theories.<sup>2,3,4</sup> The response of the liquid for the case of solid body rotation is often resolved into modes. (See Reference 3 for a detailed discussion.) This modal representation simplifies the description of the three-dimensional wave motion within the liquid. The radial mode number is  $n(1,2,3\dots)$ , and the longitudinal mode number is  $k(1,3,5\dots)$ . In order to produce a destabilizing yaw moment, the azimuthal mode number must be unity; the azimuthal mode number is implicitly understood to always be unity. As with most harmonic oscillations, only the fundamental modes (low mode numbers) are of practical importance. (Higher modes are usually damped by viscous effects.) Unfortunately, such a judgment is based upon experience or intuition for the particular problem at hand. For example, the computed data in Figure 1 were based upon  $k=5$  and  $n=1$ . It is convenient to identify a spin-up eigenfrequency history by the mode numbers  $(k,n)$  of the steady state response.

#### B. Selection of Hardware

A single occurrence of a spin-up instability was documented in Reference 11. Only a single configuration (a modified M678 with a half-caliber base,  $c/a = 4.972$ , fill ratio = 100%, and  $Re = 1.85 \times 10^6$ ) was tested. Results from a three round group indicated only one flight instability; however, the resonance time as predicted by the spin-up eigenfrequency history correlated well with the yawsonde data. The spin-up eigenfrequency history of this

- 
11. W.P. D'Amico, W. Clay, and A. Mark, "Yawsonde Data for M687-Type Projectiles With Application to Rapid Spin Decay and Stewartson-Type Spin-up Instabilities," BRL Memorandum Report ARBRL-MR-03327, June 1980 (AD A089646).

configuration (called an M687L) is shown in Figure 1 and was the basis of the selection of hardware for this present test. The (1,5) mode of Figure 1 shows a monotonically decreasing behavior with time. (Actually, for time equal to zero, the eigenfrequency is zero and a rapid increase in eigenfrequency occurs for very early times.) If the ratio of the fast precessional frequency to the spin frequency ( $\dot{\phi}_1/\dot{\phi}$ ) is equal to the spin-up eigenfrequency, then resonance occurs and a growth in yaw is possible (but is not guaranteed). Typically, an M687 projectile launched at transonic velocities will have  $\dot{\phi}_1/\dot{\phi} = 0.08$ . Hence, from Figure 1 resonance should occur for  $\tau = \dot{\phi}_1/\dot{\phi}$  at about 7 seconds. In order to produce a larger moment by forcing  $d\tau_{kn}/dt$  to be smaller, the time of the resonant matching should be larger than 7 seconds. This could be accomplished by increasing Re or c/a. An increase in either of these variables would increase the spin-up time and result in both a longer time to resonance and a smaller value of  $d\tau_{kn}/dt$ . From a practical standpoint, it would be advantageous to change c/a and then test several Re values. This approach was taken for the (1,5) mode. It was also possible to investigate the (1,3) mode by reducing the canister length. The (1,3) mode will produce the same liquid frequency as the (1,5) mode, but the effect of reduced liquid mass and lower longitudinal mode number will be observed. Figures 2 and 3 show eigenfrequency histories for (1,5) and (1,3) modes for two Reynolds numbers (1 and 50 cs oil).

Hardware was constructed for the aspect ratios shown in Figures 2 and 3. A sectioned view of a standard M687 is shown in Figure 4. Single piece canisters were fabricated utilizing M687-type components. The (1,3) canisters were constructed with the center of the cavity in the middle of the payload section with very thick endwalls. Bases with quarter-caliber boattails (typical of the standard M483A1 family of shell) were utilized, rather than the half-caliber boattails that were used for the M687L shell. Table 1 lists the projectile types and pertinent physical characteristics.

TABLE 1. PROJECTILE/CANISTER DESCRIPTIONS

Projectile Type	Year	Boattail		a (cm)	$m_L a^{2*}$ (kg·m <sup>2</sup> )	Fill Ratio (%)
		(cal)	c/a			
M687	1974	1/4	4.390	5.37	0.012	80
XM687L	1978	1/2	4.973	5.37	0.014	100
XM679A	1982	1/4	5.200	5.14	0.012	100
XM687B	1982	1/4	3.120	5.14	0.007	100

\*Based upon the density of water and for a fill ratio of 100%.

### III. RESULTS

#### A. Test Site

A test program was conducted at NASA Wallops Island (WI), Virginia, during September 1982. A ground receiving station was operated by BRL on the Pad 2 launch site. Radar tracking and backup telemetry coverage were provided by WI personnel. An M185 tube with a standard muzzle break was used in a universal mount. Launch velocities were obtained by smear cameras. Table 2 gives a round-by-round summary of the test program. All projectiles were fitted with fuze-configured yawsondes.<sup>12</sup> Yawsonde data are in the form of solar aspect angle ( $\Sigma$ , which is related to the peak-to-peak yawing motion about the trajectory) and time rate of change of the Eulerian roll angle,  $\dot{\phi}$  (when the yaw is small  $\dot{\phi}$  is nearly the spin; the data are simply labeled spin). The yawing motion of the projectile consists of two modes of precession, fast and slow. Typical values for the fast and slow modes (at transonic launch velocities for 155mm shell) are 10 and 1 Hz, respectively. The amplitude of the fast precessional mode is destabilized by the liquid payload.

TABLE 2. ROUND-BY-ROUND SUMMARY<sup>a</sup>

Date	Round Type	BRL Number	WI Number	Muzzle Velocity (m/s)	Projectile Mass (kg)	Range (m)	FMA <sup>b</sup> (deg)	Resonant <sup>c</sup> Time (sec)
23 Sep 82	A1-1	1649	E1-397	352.7	35.6	8,549		---
23 Sep 82	A1-2	1765	E1-398	351.7	35.7	8,686	4	3.0
23 Sep 82	A1-3	1775	E1-399	353.6	35.7	8,961	3.5	---
29 Sep 82	A1-4	1808	E1-402	352.3	35.8	9,052	1.5	5.0
29 Sep 82	A50-1	1810	E1-403	348.7	36.4	8,793	1.5	5.0
29 Sep 82	B1-1	1814	E1-405	353.3	34.7	8,779	1.0	4.0
29 Sep 82	B1-2	1815	E1-406	354.5	34.8	8,671	1.0	3.5
29 Sep 82	B1-3	1816	E1-407	353.9	34.7	8,595	1.5	4.0
29 Sep 82	B50-1	1848	E1-408	352.3	35.3	8,869		---

<sup>a</sup> All rounds were launched at a quadrant elevation of 750 mils with charge 4W.

<sup>b</sup> FMA is defined as half of the first maximum amplitude observed within the yawsonde data.

<sup>c</sup> Time at which growth of the fast mode precession was observed within the yawsonde data.

12. W. H. Mernagen and W. H. Clay, "The Design of a Second Generation Yawsonde," BRL Memorandum Report ARBRL-MR-2358, April 1974 (AD 780064).

## B. Yawsonde Data

Table 3 lists the number of unstable rounds within each group. (Also listed are Reynolds numbers and viscosities.) The data will be discussed by projectile type: A and B.

TABLE 3. NASA WALLOPS ISLAND TEST -- SEPTEMBER 1982

Projectile Type	Viscosity (cs)	Re	Rounds Tested Unstable/Total
XM687A	1	$1.99 \times 10^6$	3/4
XM687A	50	$3.98 \times 10^4$	1/1
XM687B	1	$1.99 \times 10^6$	3/3
XM678B	50	$3.98 \times 10^4$	0/1

### 1. Type A Projectiles

Figures 5a and 5b show limited yawsonde data for Round A1-1. The telemetry data contain spurious pulses of noise producing erroneous yaw data. (Spin data were not sensitive to the noise.) It is clear, however, that a small launch yaw existed and larger yaw resulted downrange. No large reduction in spin was observed. Figures 6a, 6b, and 6c give the yawsonde data for Round A1-2. Upon launch the yaw was dominated by the slow precessional mode. The amplitude of the fast precessional mode decayed until approximately 3 seconds where growth was seen. The slow mode then damped, while the fast mode slowly grew to an amplitude of 5 degrees at 15 seconds. During the remainder of the flight, the fast mode continued to grow, but catastrophic levels of yaw were not observed. The spin data show a modulation (characteristic of yawing projectiles), but large despin did not occur. Figures 7a, 7b, and 7c show data for Round A1-3. This round was stable. However, within Figure 7b the fast precessional mode damps between 0-2.5 seconds and then grows slightly in the 2.5-15 second time frame. The fast mode damped during the down leg of the trajectory unlike the previous two rounds. No other anomalies were noted. The data for Round A1-4 are given in Figures 8a, 8b, and 8c. These data are essentially identical to Round A1-2. Very early data indicate a small FMA of 1.5 degrees that is dominated by the fast mode. (Typically, the early yaw contains both slow and fast modes and is slightly dominated by the slow mode.) The fast mode damped subsequent launch and began to grow at approximately 5 seconds. Figures 9a, 9b, and 9c show data for the only 50 cs projectile, Round A50-1. The data were very similar to the previous unstable rounds which were loaded with 1 cs oil. The very early yaw was dominated by the fast mode, which rapidly damped and then grew beginning at about 5.0 seconds. No unusual spin data were observed.

## 2. Type B Projectiles

Figures 10a, 10b, and 10c show the yawsonde data for Round B1-1. Early data show an FMA of 1.0 degree with rapid damping for the fast precessional mode. The fast mode then dramatically grew at approximately 4.0 seconds and resulted in a yaw amplitude of 5 degrees. The spin data were similar to the A series shell. Figures 11a, 11b, and 11c give yawsonde data for Round B1-2. The initial yawing motion was small (FMA = 1.0 degree and dominated by the slow mode), but the fast precession began to increase at 3.5 seconds. These data were very similar to Round B1-1. Data for Round B1-3 are given in Figures 12a, 12b, and 12c. An FMA of 1.5 degrees was observed, and the fast precessional mode began to increase in amplitude at approximately 4.0 seconds. The spin data were typical of the previous rounds. Data for the 50 cs projectile in this series are in Figures 13a and 13b. No unusual yaw or spin behavior was noted.

## IV. DISCUSSION

A short description of the spin-up analysis by Murphy<sup>10</sup> will be presented prior to a discussion of the data. The equations governing the liquid eigenfrequencies during spin-up indicate the presence of a critical layer within the flow domain. This critical layer is a region where the local oscillation frequency (during the spin-up process) matches the rotational velocity of the main azimuthal flow. Considerable effort must be expended to properly treat the critical layer, but Murphy has suggested a model that is applicable when the critical layer is not a dominant factor. This model can be used to compute yaw moments during spin-up except at early times. (This is usually where the critical layer is important.) Flight data for the 50 cs rounds can be treated by this theory, while the higher Re cases will require a more complete theory. It must also be stated that the present spin-up analysis has been linearized for small amplitudes and is a quasi-steady state approach that does not reflect unsteady effects such as the coning history, etc. Qualitative comparisons between this spin-up theory and the flight data should be made as a guide to the development of more complete analyses and as a basis for future flight tests.

Assuming only the fast yaw mode is important, the liquid moment is assumed to have the following form.

$$\text{Liquid Moment} = m_L a^2 \dot{\phi}^2 \tau_1 K_1 e^{i\phi} (C_{LSM_1} + i C_{LIM_1}) \quad (3)$$

Both moment coefficients can be computed during spin-up by the methods within Reference 10, but the projectile yaw is controlled only by  $C_{LSM_1}$ . Computed results are shown in Figures 14a and 14b for the A-50 and B-50 cases (for  $c/a = 5.20$  and  $c/a = 3.12$  at  $Re = 3.98 \times 10^4$ ). The independent variable shown is  $\phi = \dot{\phi}t$ , the roll angle from time zero.  $C_{LSM_1}$  is a function of the yaw growth rate and the coning frequency. These calculations for  $C_{LSM_1}$  are for  $\tau = 0.090$ . The solid lines are the total moment coefficient due to both pressure

and viscous effects, while the dashed lines indicate only the part due to pressure. The area under the curve in Figures 14a or 14b represents the angular impulse per radian or

$$\int \left( \frac{\text{Liquid Moment}}{K_1} \right) dt = m_L a^2 \dot{\phi}^2 \tau_1 \int C_{LSM_1} d\phi \quad (4)$$

In a qualitative sense, the flight data suggest that the unstable A series should have a larger angular impulse than the stable B series. The angular impulse should be computed over the same time domain for such a comparison; however, this was not possible. The presence of the critical layer prevented proper estimations for  $C_{LSM_1}$  over the same times for both aspect ratios.

Hence, a simpler criterion was sought. It is assumed that in the actual flight case only the angular impulse due to the local maxima in  $C_{LSM_1}$  is impor-

tant. This could be justified somewhat since aerodynamic damping has been omitted, but admittedly a complete angular impulse curve would be preferable. A simple criterion can be established by the use of a so-called "quality factor" or "Q," which is quite common in the analysis of circuit resonances in electrical engineering. The bandwidth of the resonance is determined from 0.707 times the maximum response. In the problem at hand, the Phi intercepts for 0.707 ( $C_{LSM_1}$ ) max are easily found. The bandwidths, B, are

shown on Figures 14a and 14b. The areas under each curve (as defined by the bandwidth) were measured and were found to be approximately equal. The actual moment then scales as  $m_L a^2 \dot{\phi}^2 \tau_1$ . For  $c/a = 5.20$  the total moment experienced during spin-up would be larger than for  $c/a = 3.12$ , since all quantities are the same except for  $m_L$ .

A summary of computed and observed data is presented in Table 4. The computed resonance time was selected at the spin-up eigenfrequency of 0.091. This value of  $\dot{\phi}_1/\dot{\phi}$  (fast precessional frequency/spin frequency = 10 Hz/110 Hz) was taken as a nominal value for all rounds.

Qualitative agreement was found between the computed times for resonance and the observed times for yaw growth for the first three cases. For the B-50 cs case where  $d\tau_{kn}/dt$  was the steepest, yaw growth was not observed, which is qualitatively correct. It is interesting to note that the reduction in the liquid mass for the B series did not yield stable flights for the higher Reynolds number case. However, the reduction in the liquid mass and a larger value of  $d\tau_{kn}/dt$  (caused by a lower Re value) produced a stable flight for the single B-50 cs round. This is in qualitative agreement with Murphy's spin-up moment calculation. In general, the observed unstable yaw behavior was not catastrophic nor were range losses extreme. However, the yaw that was experienced is unacceptable in that the drag is increased compared to the drag of solid payload rounds with the same exterior shape. It is possible that

a slight reduction in the aerodynamic damping (perhaps stimulated by a lower atmospheric density or a half caliber boattail) would have produced large yaw and substantial range losses. Although the projectile sample sizes were very small, it was encouraging that the projectile flight behavior (stable or unstable) was uniform.

TABLE 4. COMPARISON OF COMPUTED AND OBSERVED DATA

Aspect Ratio	Round Type	Computed Time (Sec)	Resonant Time (Sec)	Reynolds Number	$d\tau_{kn}/dt$	Number of Rounds Unstable/Total
5.200	A-1	2-3	3-5	$1.99 \times 10^6$	-0.008	3/4
5.200	A-50	2-3	5	$3.98 \times 10^6$	-0.44	1/1
3.200	B-1	5-6	3.5-4	$1.99 \times 10^6$	-0.013	3/3
3.200	B-50	1-2	-----	$3.98 \times 10^6$	-0.66	0/1

#### V. CONCLUSIONS

A liquid-filled projectile can become unstable due to a resonance between the fast precessional frequency and a liquid eigenfrequency. During the liquid spin-up process when the eigenfrequency varies slowly, the destabilizing moment can become large. Conversely, if the eigenfrequency varies rapidly with time, then resonance effects are reduced and destabilizing moments may be avoided. With the use of a spin-up eigenfrequency code, projectile hardware was designed and tested to investigate these effects. Flight data were in qualitative agreement with the eigenfrequency estimates and indicated that the magnitude of spin-up moments can be reduced by a rapid time variation of the liquid eigenfrequency in the vicinity of resonance. An approximate spin-up theory was applied to two flight cases and was also in qualitative agreement.

#### ACKNOWLEDGMENTS

The author is indebted to many people: to Mr. N. Surratt and Mr. C. Lamka for the fabrication and loading of these shell, to Free FLIGHT Aeroballistic Branch personnel for conduct of the test and data reduction, to Ms. J. M. Bartos for computation of spin-up eigenfrequency histories, and to Dr. C. H. Murphy and Mr. J. W. Bradley for calculations of yaw moment during spin-up. Finally, the Wallops Flight Center (NASA) personnel are commended for their technical and administrative support of this test. Mr. R. Atkins of WI NASA devoted a great deal of time and effort to aid us in the successful and timely conduct of this program.

# SPIN-UP EIGENFREQUENCY M687L

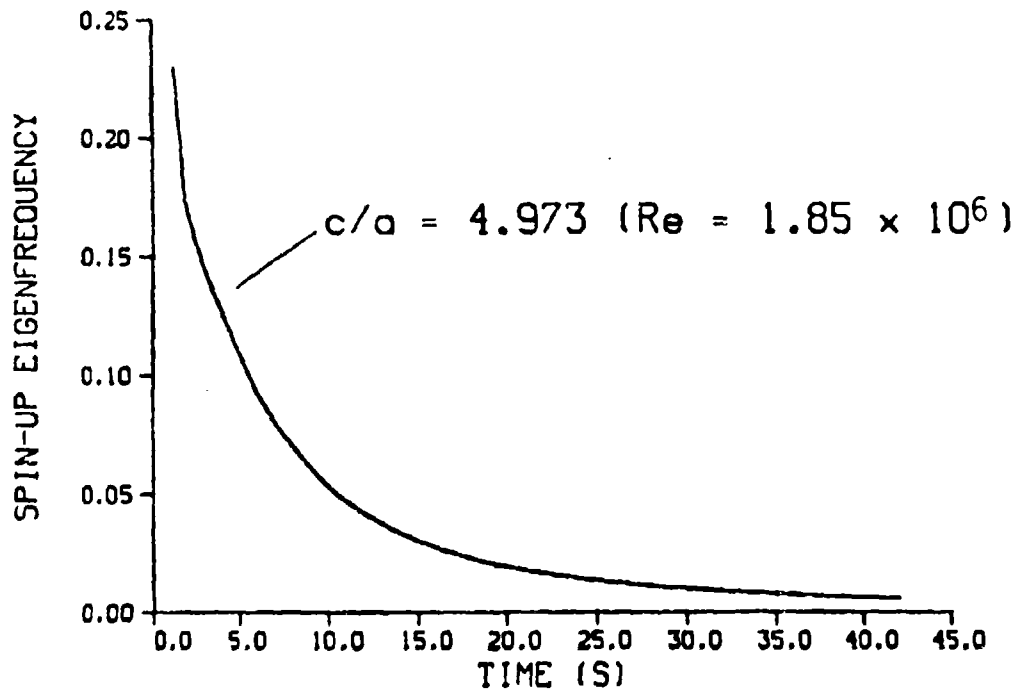


Figure 1. Spin-Up Eigenfrequency History for an M687L  
(k = 7, n = 1).

SPIN-UP EIGENFREQUENCY  
M687A1  
M687A50

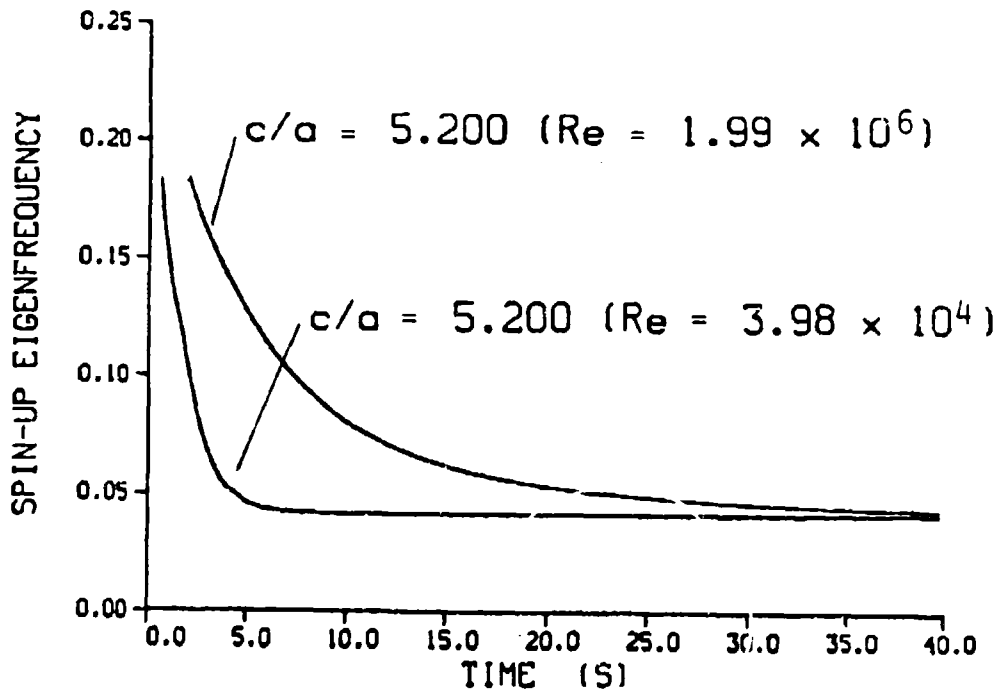


Figure 2. Spin-Up Eigenfrequency Histories for an M687A  
( $k = 7, n = 1$ ).

SPIN-UP EIGENFREQUENCY  
M687B1  
M687B50

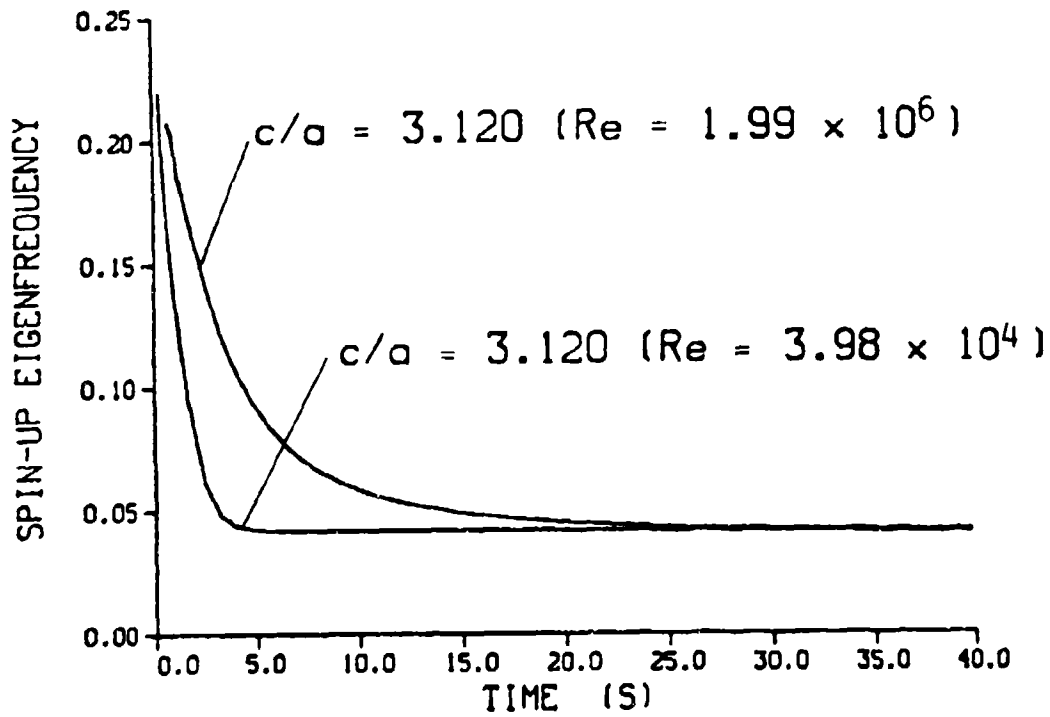


Figure 3. Spin-Up Eigenfrequency Histories for an M687B  
( $k = 5, n = 1$ ).

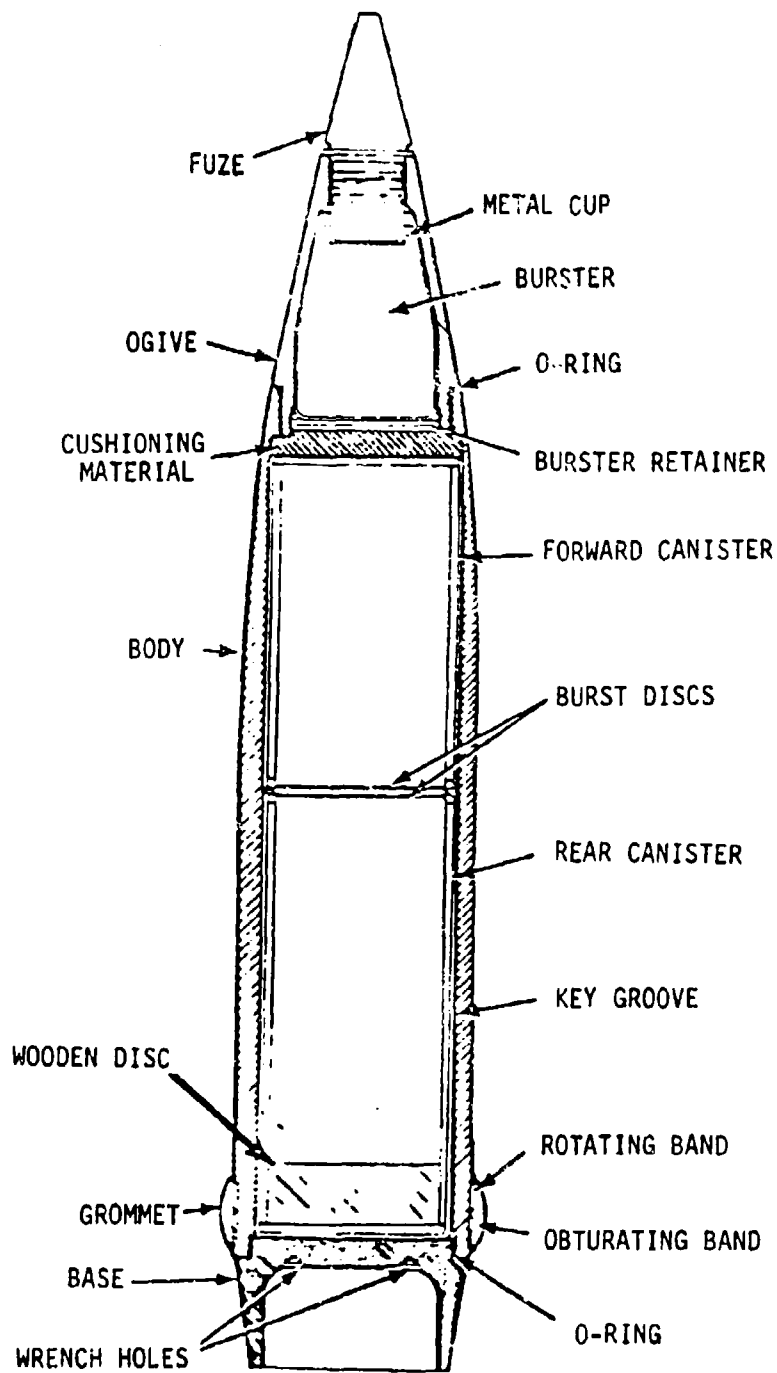


Figure 4. Sectioned View of a Standard M687,  
155mm, Binary Projectile.

SITE I. D. HALLOPS BRL ROUND1649 FIRED 09-23-82

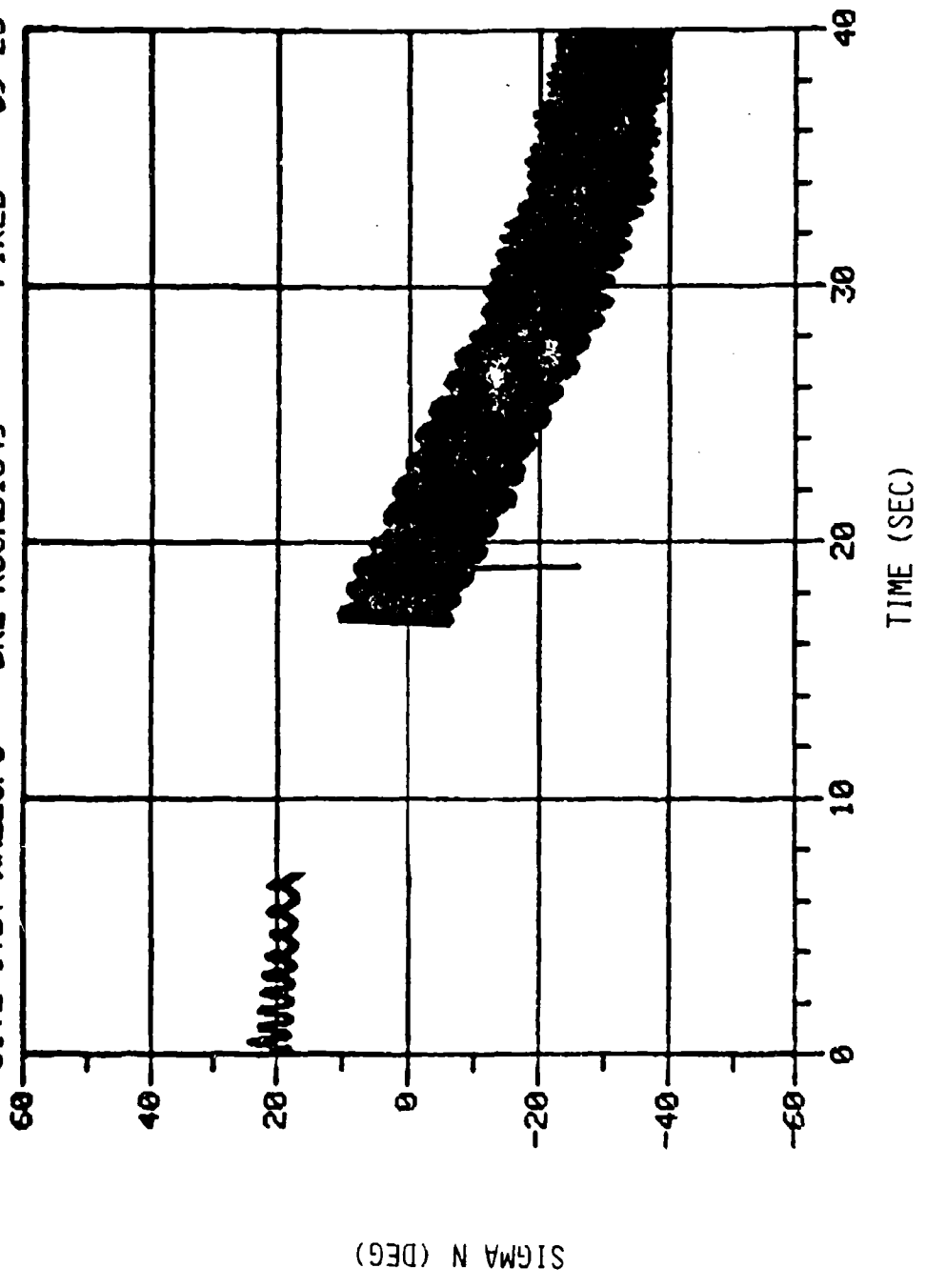


Figure 5a. Sigma N Versus Time for A1-1.

SITE I. O. WALLEPS    BRL ROUND1649    FIRED    09-23-82

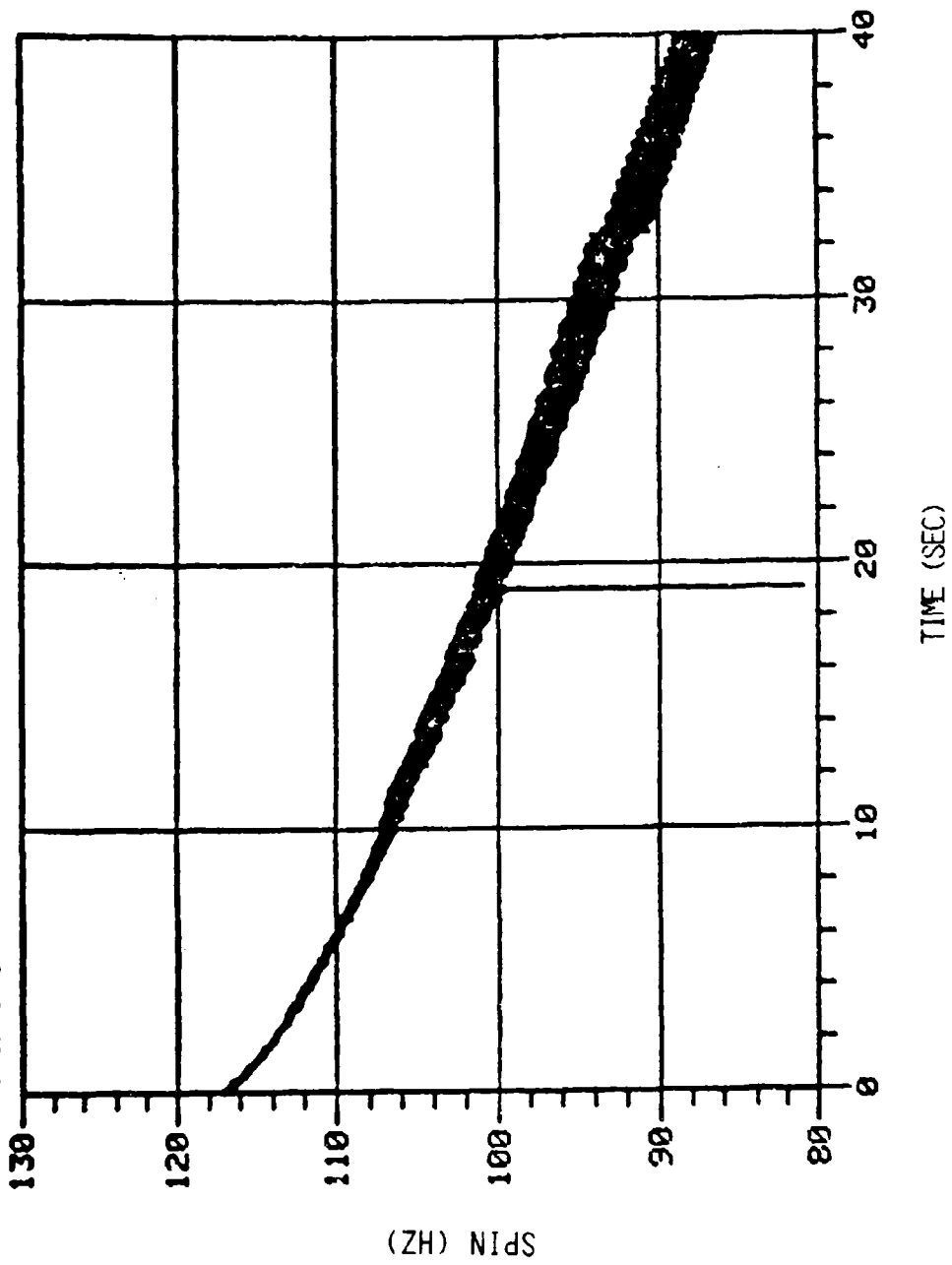


Figure 5b. Spin Versus Time for A1-1.

SITE I.D. WALLEPS BRL ROUND1765 FIRED 09-23-82

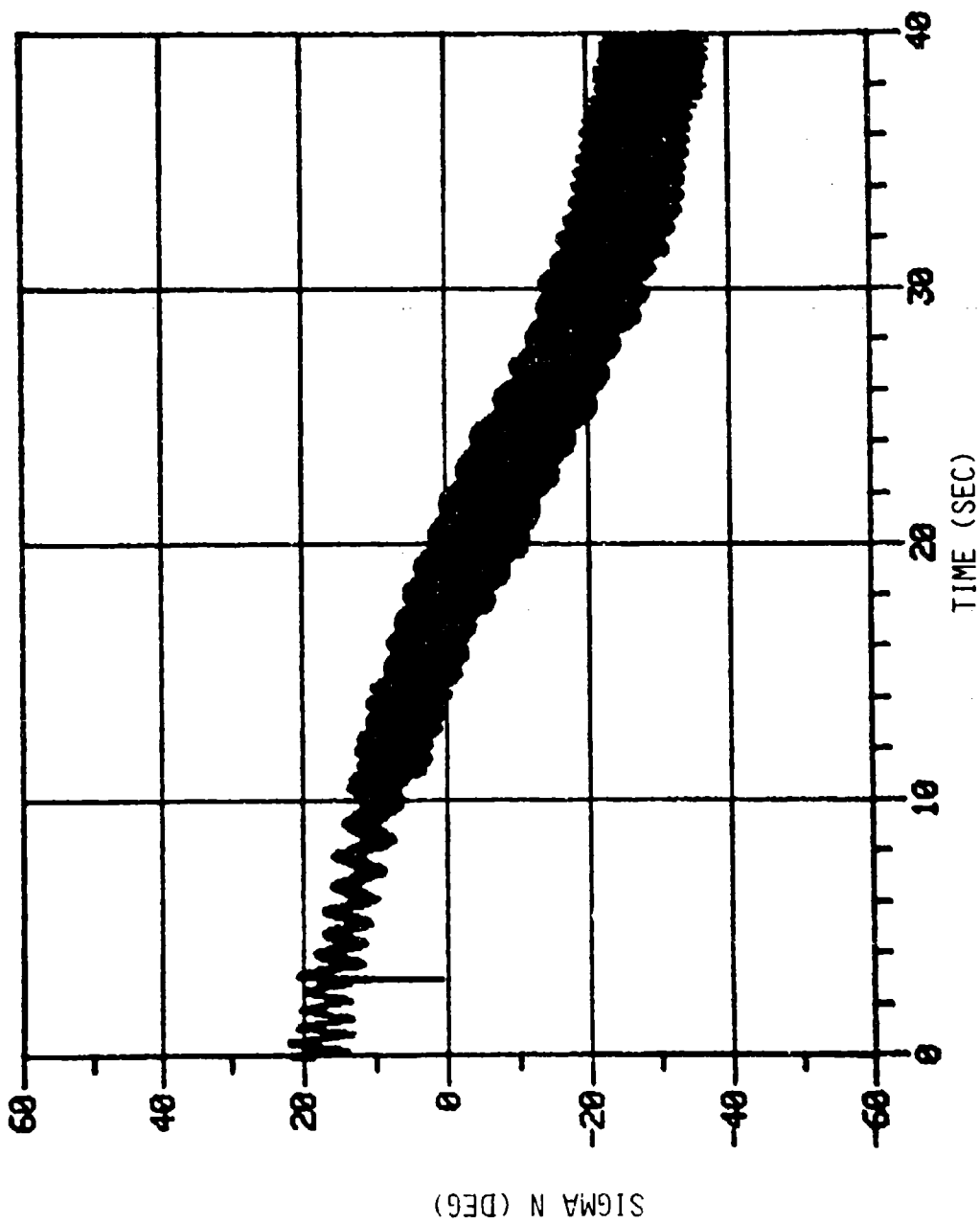
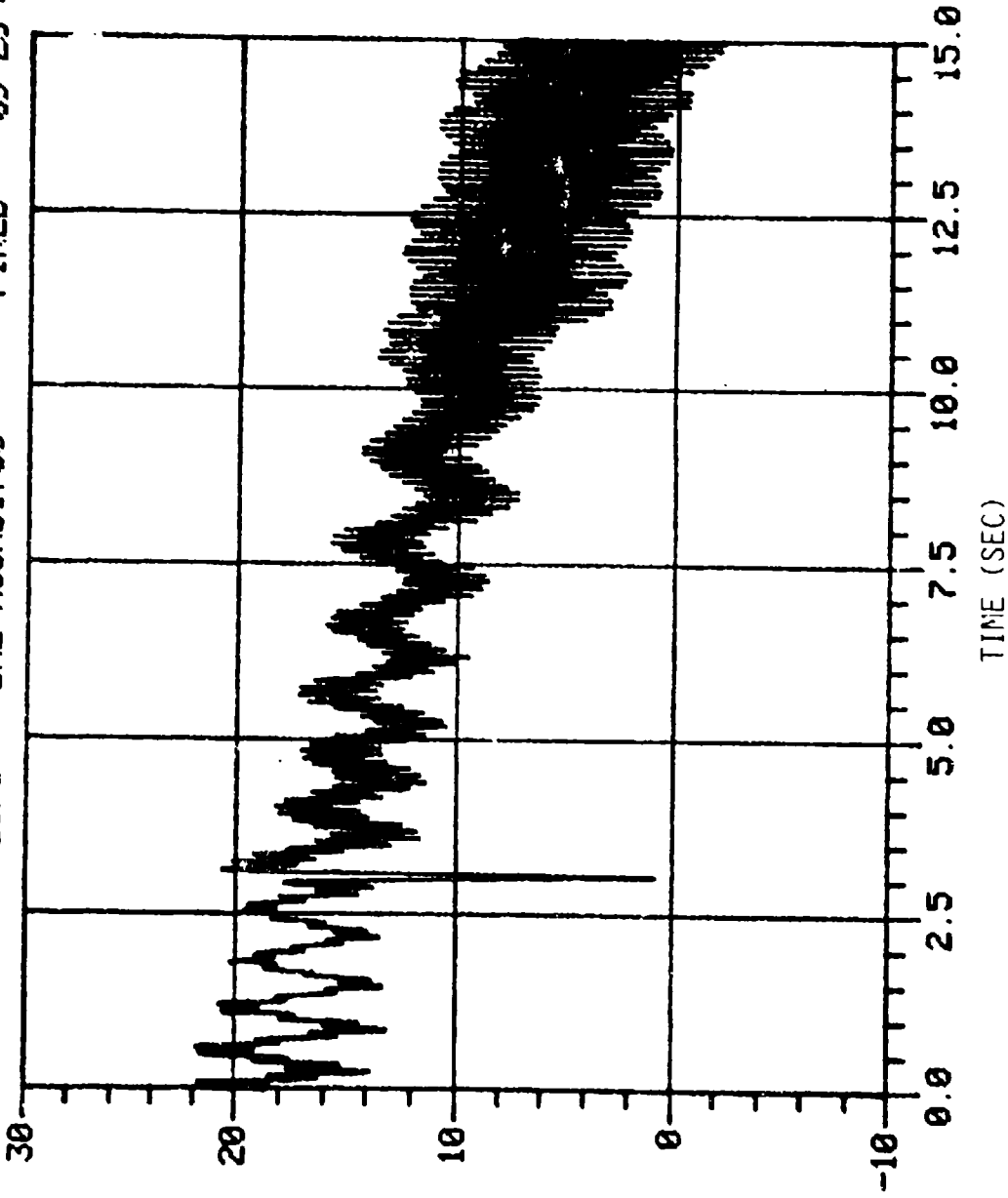


Figure 6a. Sigma N Versus Time for A1-2 (0-40 Sec).

SITE I.O. WALLEPS BRL ROUND1765 FIRED 09-23-82



SIGMA N (DEG)

TIME (SEC)

Figure 6b. Sigma N Versus Time for A1-2 (0-15 Sec).

SITE I.O. WALLOPS BRL ROUND1765 FIRED 09-23-82

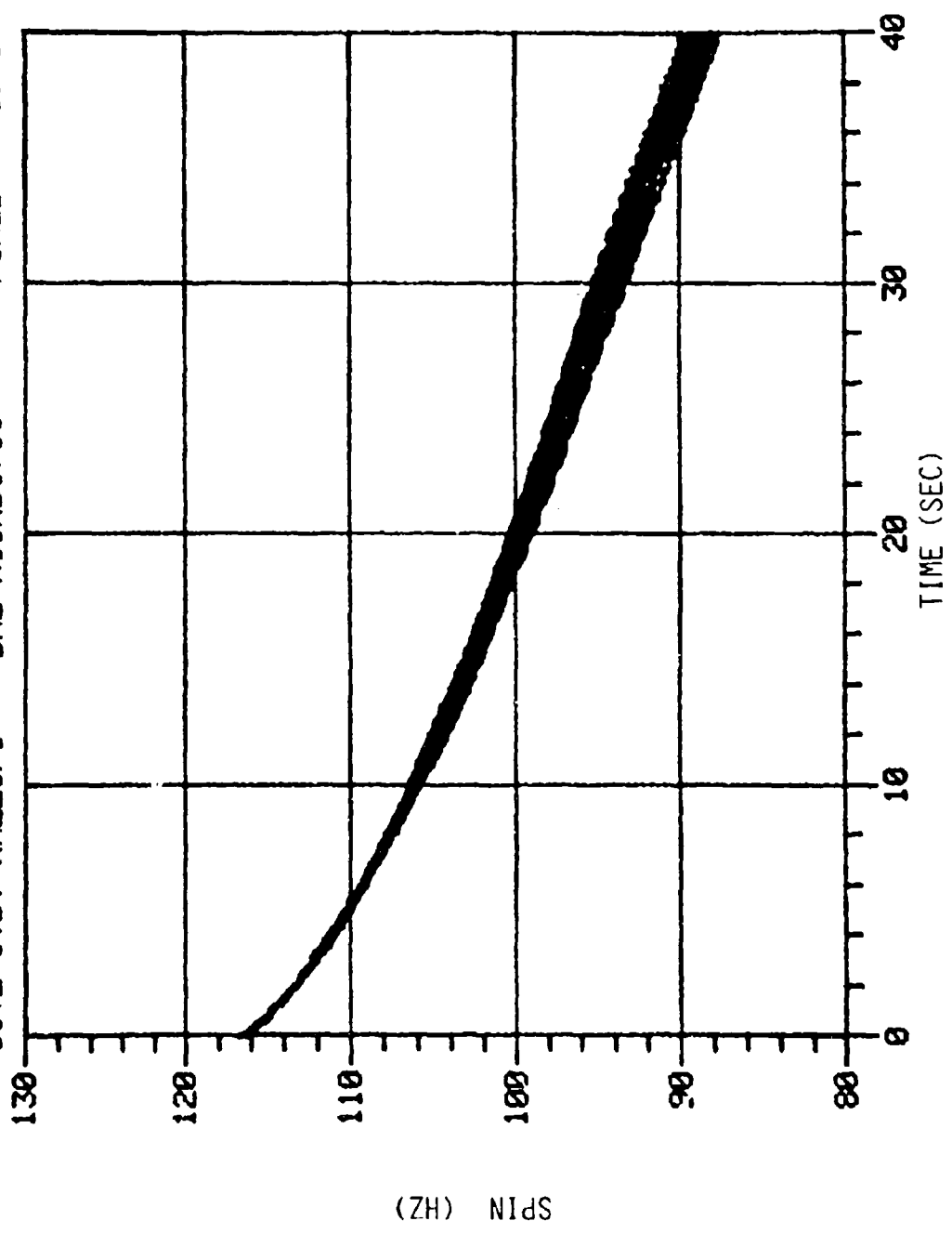


Figure 6c. Spin Versus Time for A1-2.

SITE I.D. WALLEPS BRL ROUND1775 FIRED 09-23-92

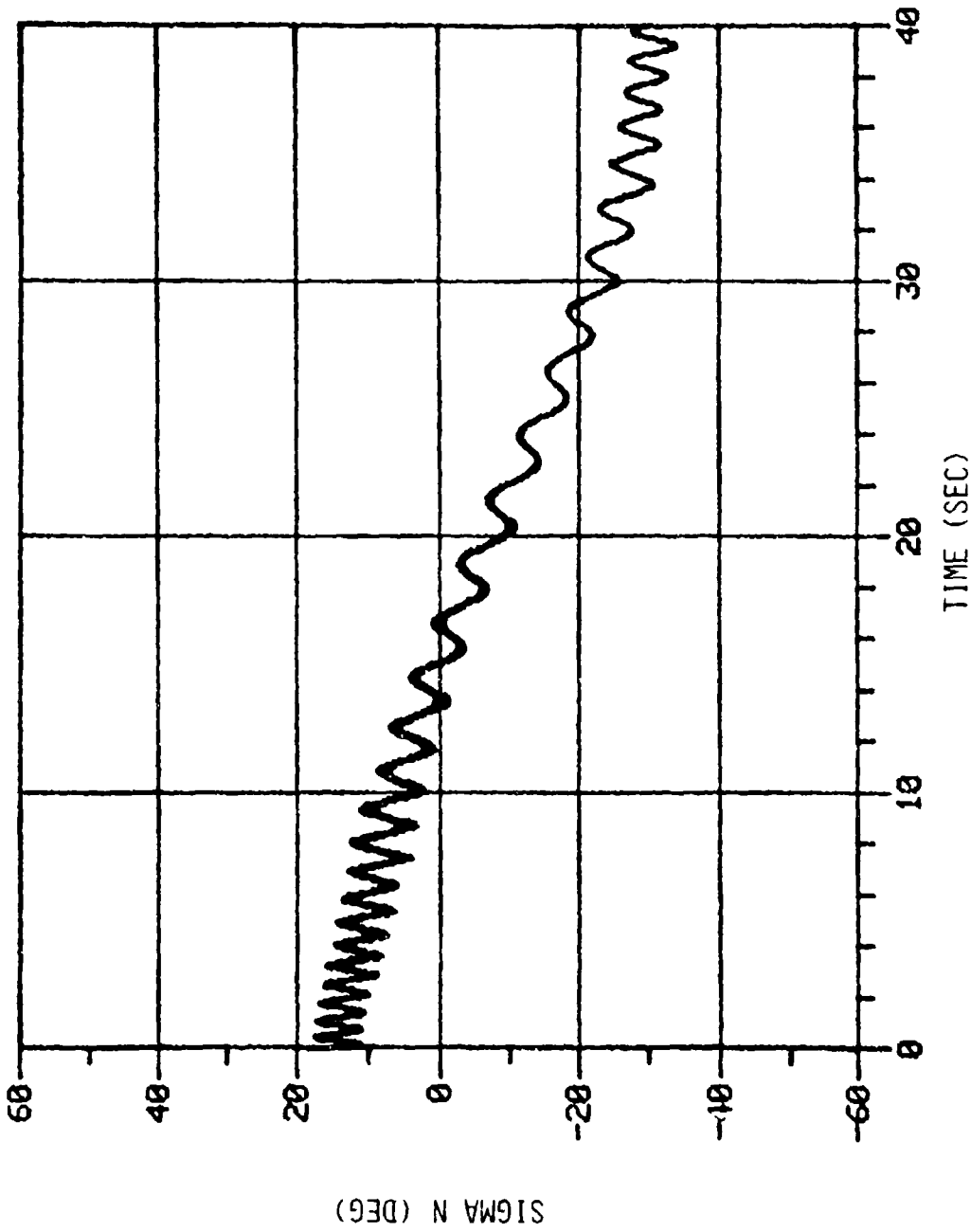


Figure 7a. Sigma N Versus Time for A1-3 (0-40 Sec).

SITE I.O. WALLEPS BRL ROUND175 FIRED 09-23-62

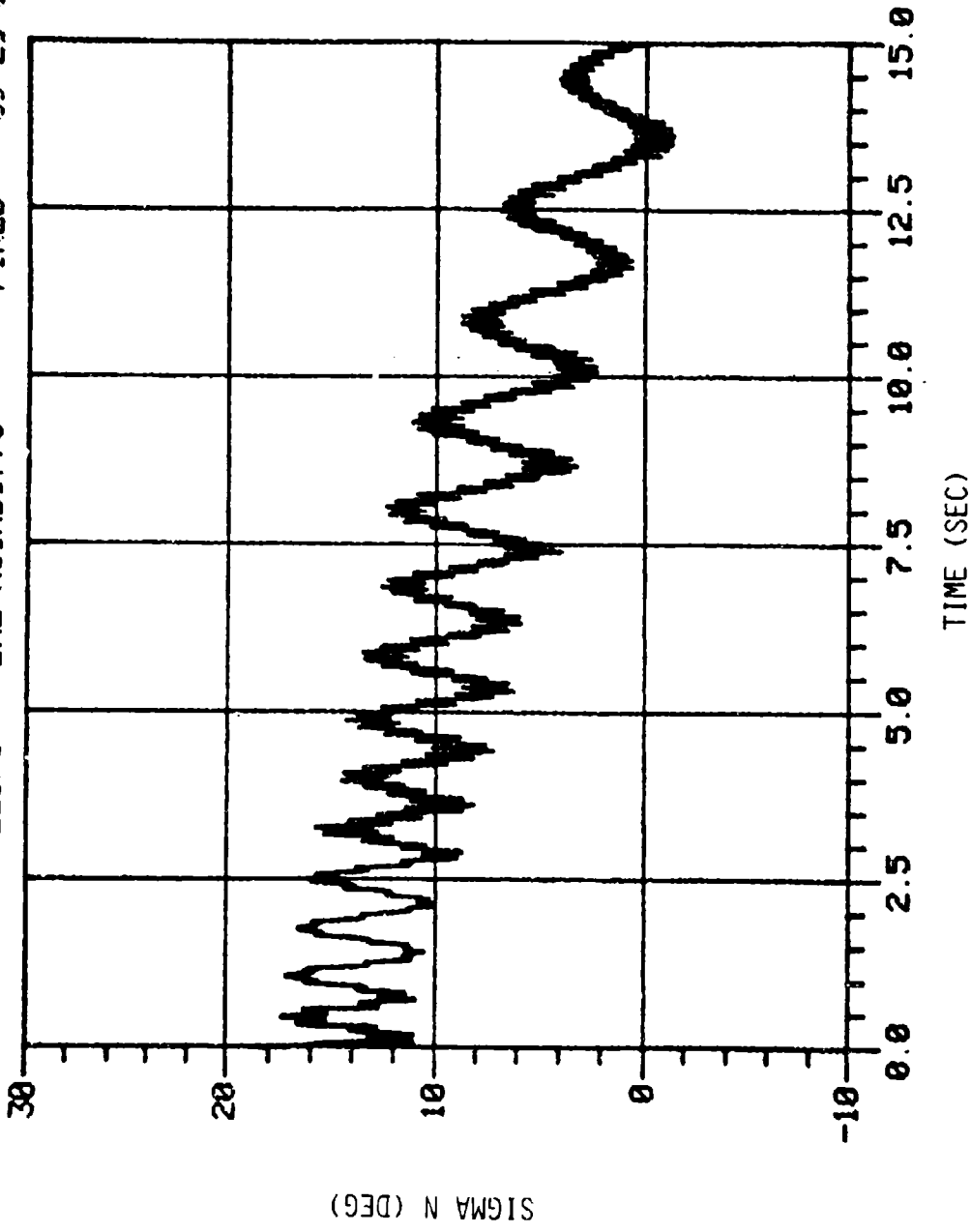


Figure 7b. Sigma N Versus Time for A1-3 (0-15 Sec).

SITE I. D. WALLEOPS BRL ROUND1775 FIRED 09-23-82

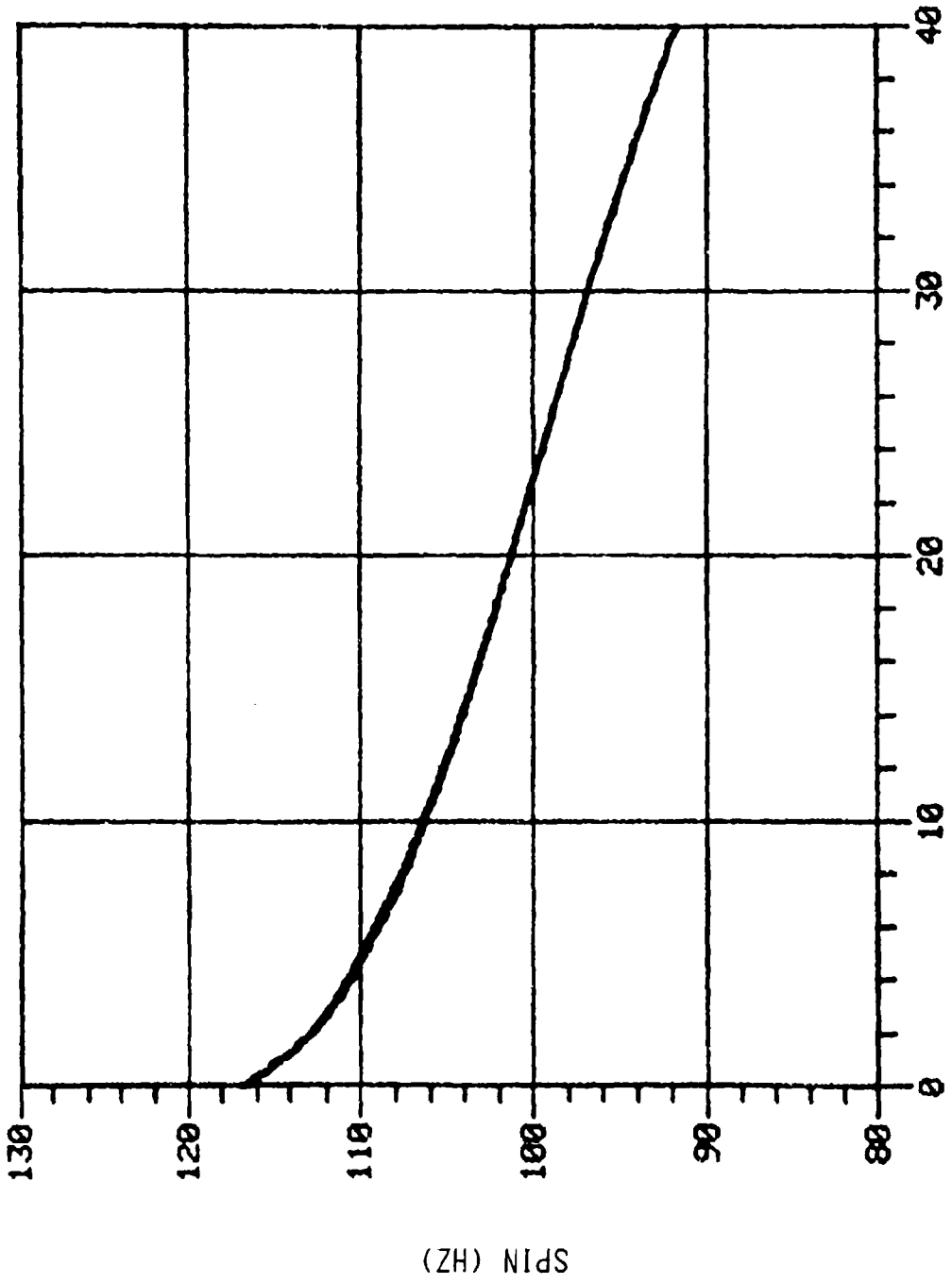


Figure 7c. Spin Versus Time for A1-3.

SITE I.D. WALLOPS BRL ROUND1808 FIRED 09-29-82

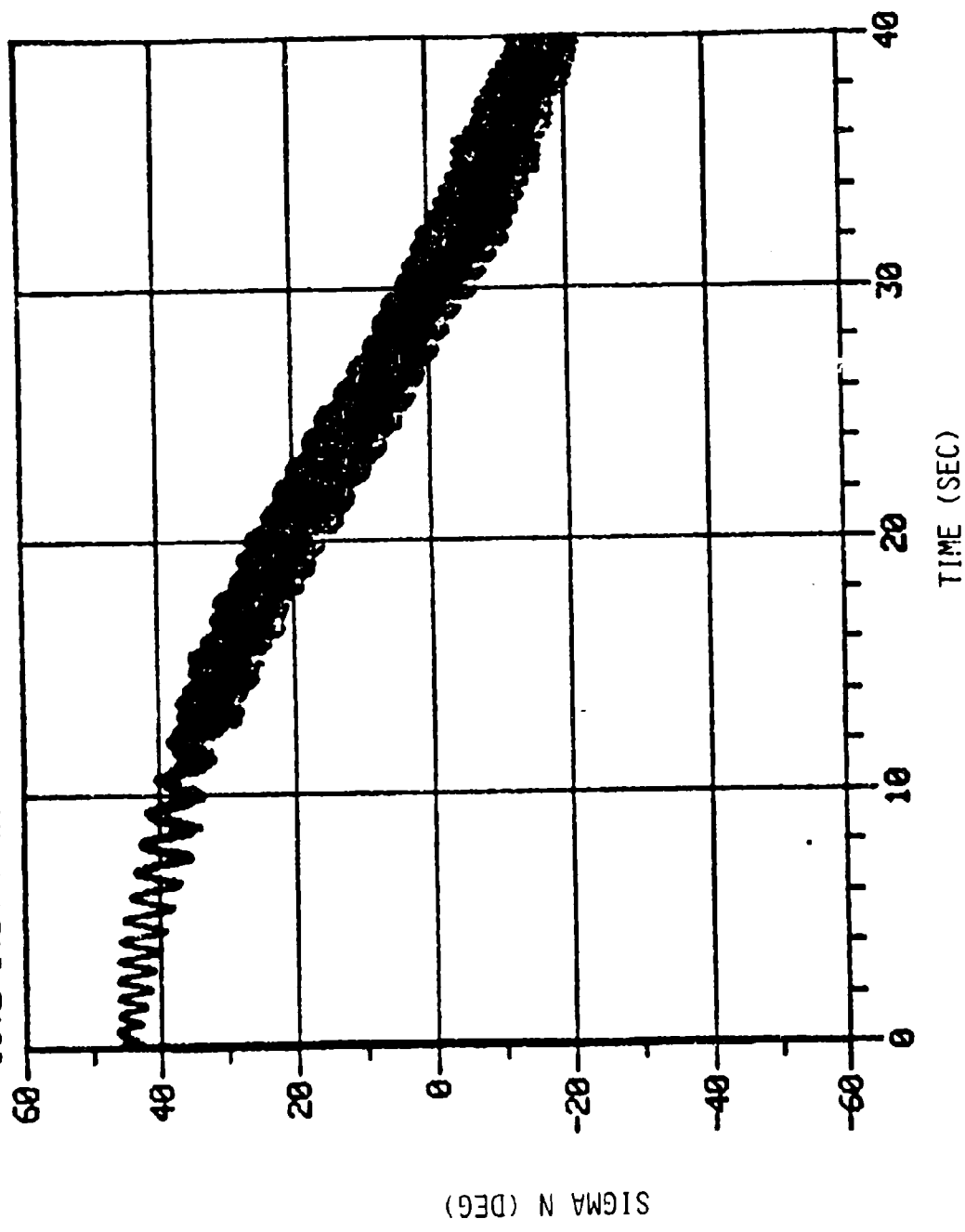


Figure 8a. Sigma N Versus Time for Ai-4 (0-40 Sec).

SITE I. D. WALLEPS

BRL ROUND1808

FIRED

99-29-82

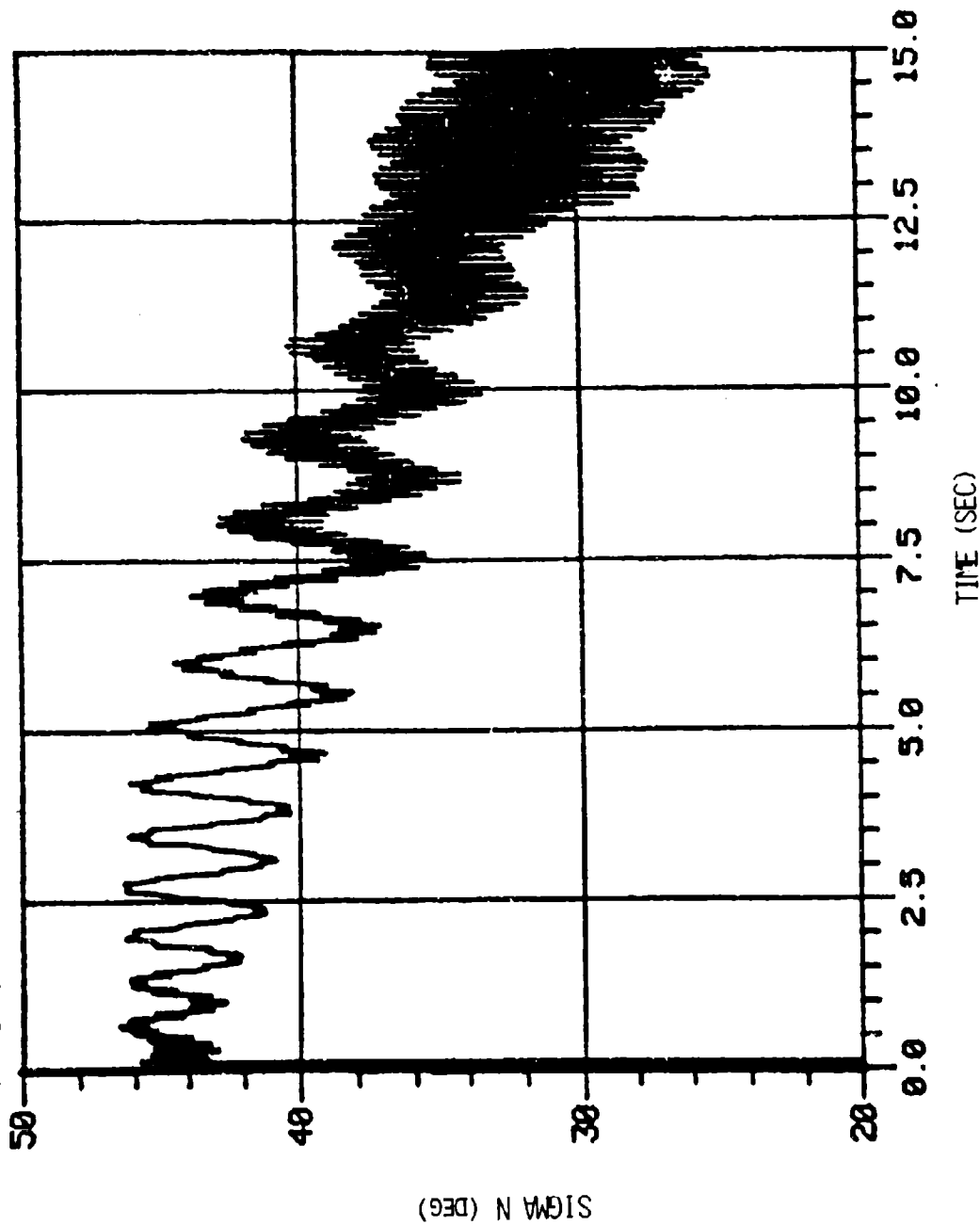


Figure 8b. Sigma N Versus Time for A1-4 (0-15 Sec).

SITE I. D. WALLOPS BRL ROUND1898 FIRED 09-29-82

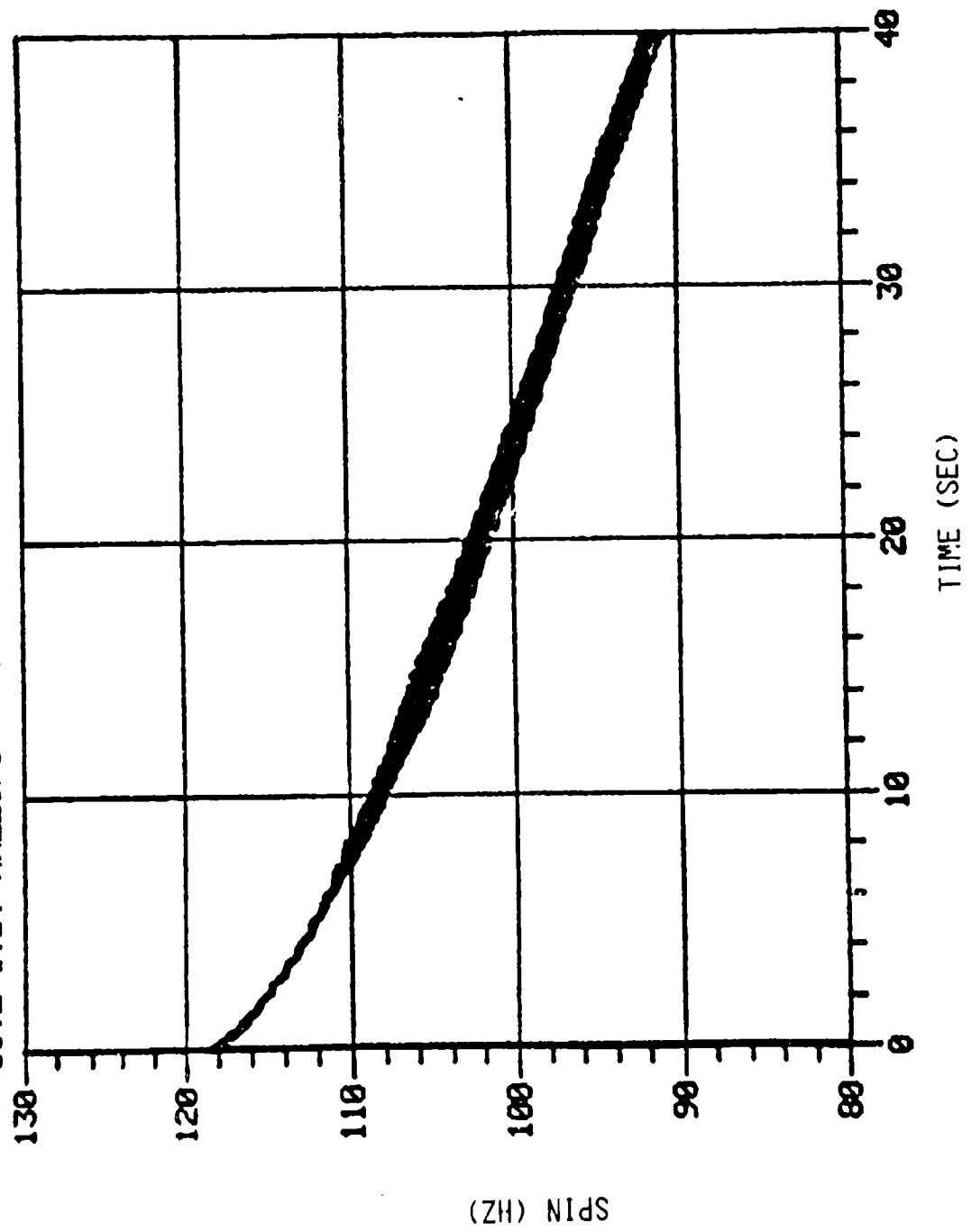


Figure 8c. Spin Versus Time for Al-4.

SITE I.D. WALLEPS

FIRE

BRL ROUND1810

09-29-82

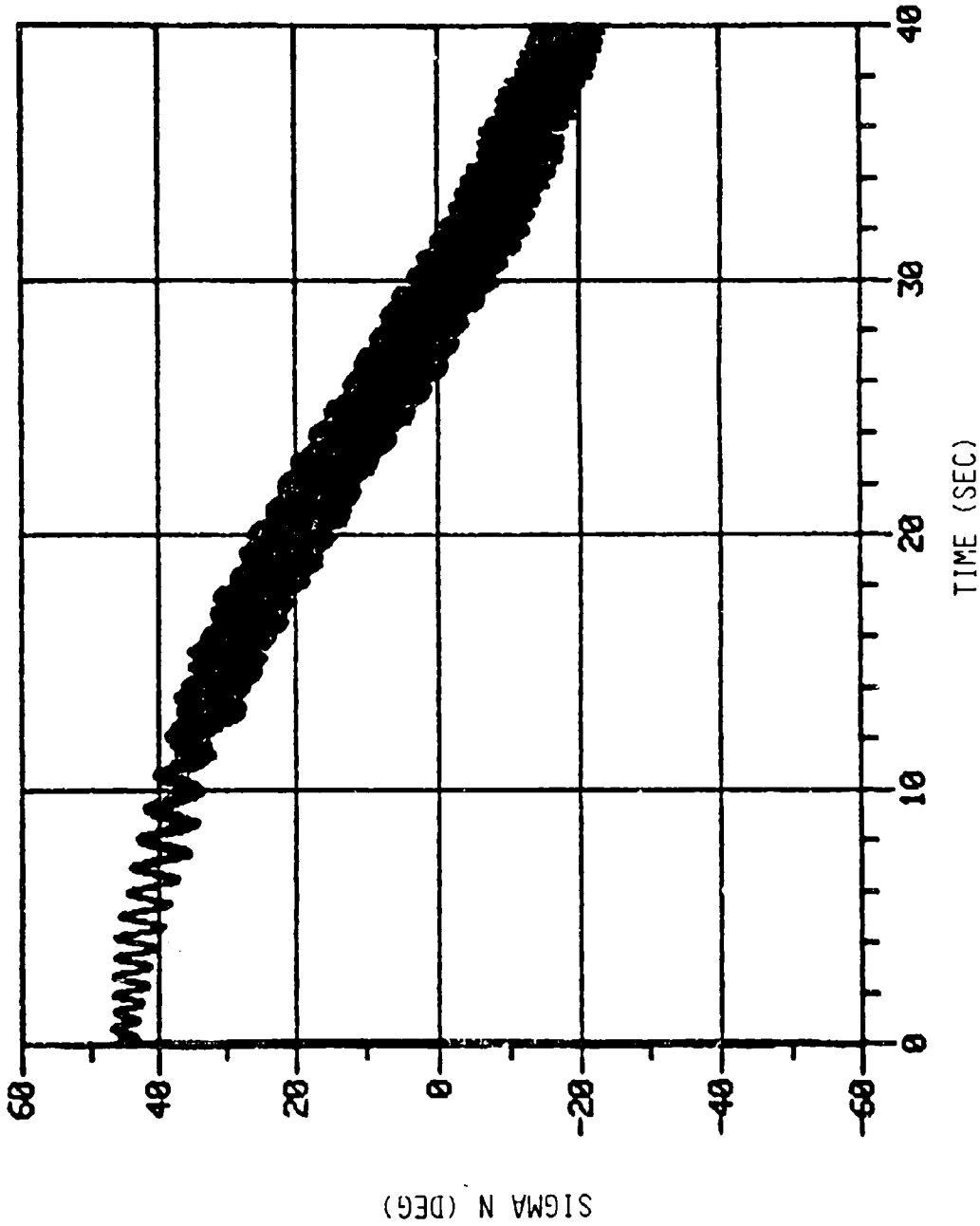


Figure 9a. Sigma N Versus Time for A50-1 (0-40 Sec).

SITE I.D. WALLEPS BRL ROUND1810 FIRED 09-29-82

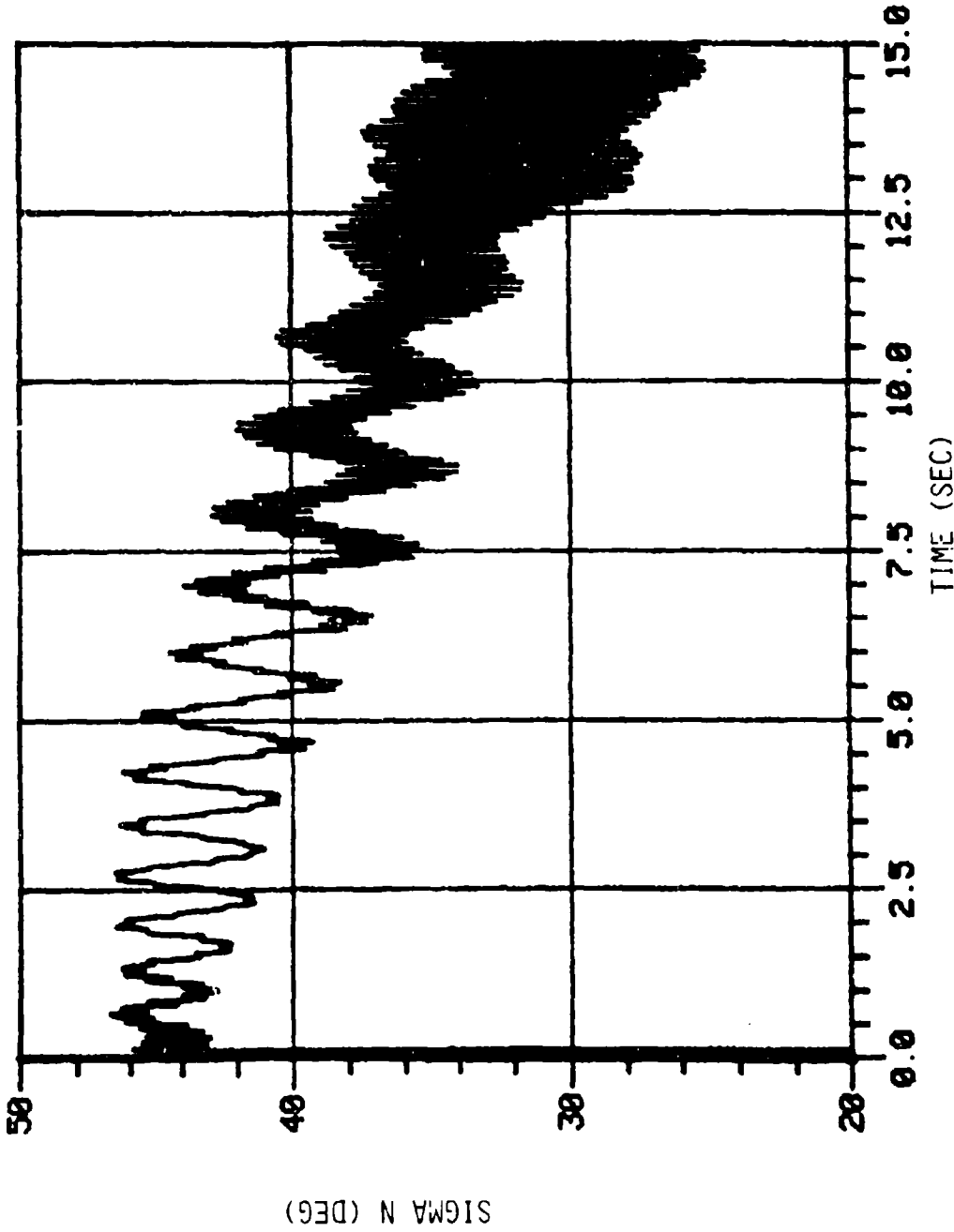


Figure 9b. Sigma N Versus Time for A50-1 (0-15 Sec).

SITE I.O. HALLOPS BRL ROUND1810 FIRED 09-29-82

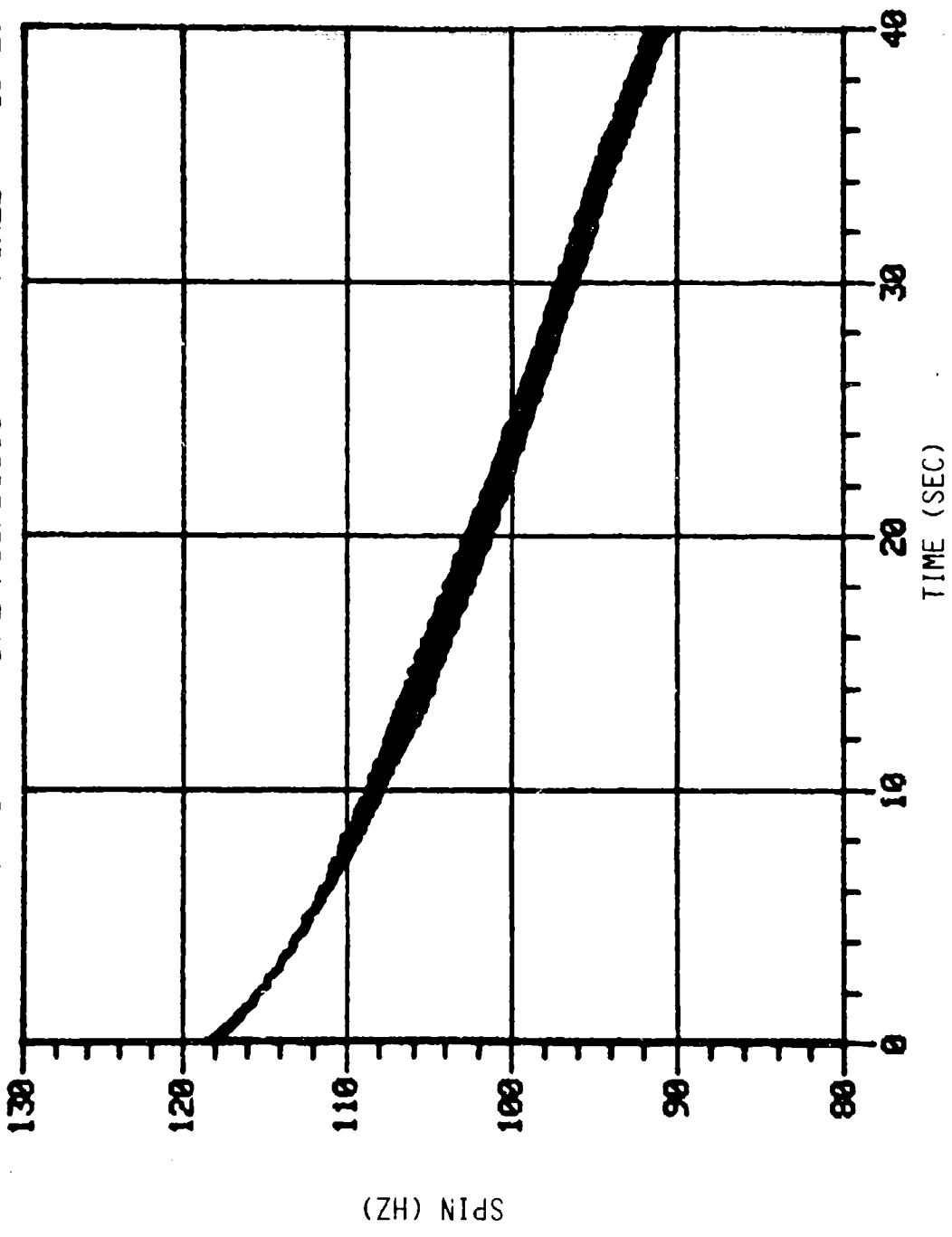


Figure 9c Spin Versus Time for A50-1.

SITE I. D. WALLEPS BRL ROUND 1814 FIRED 09-29-62

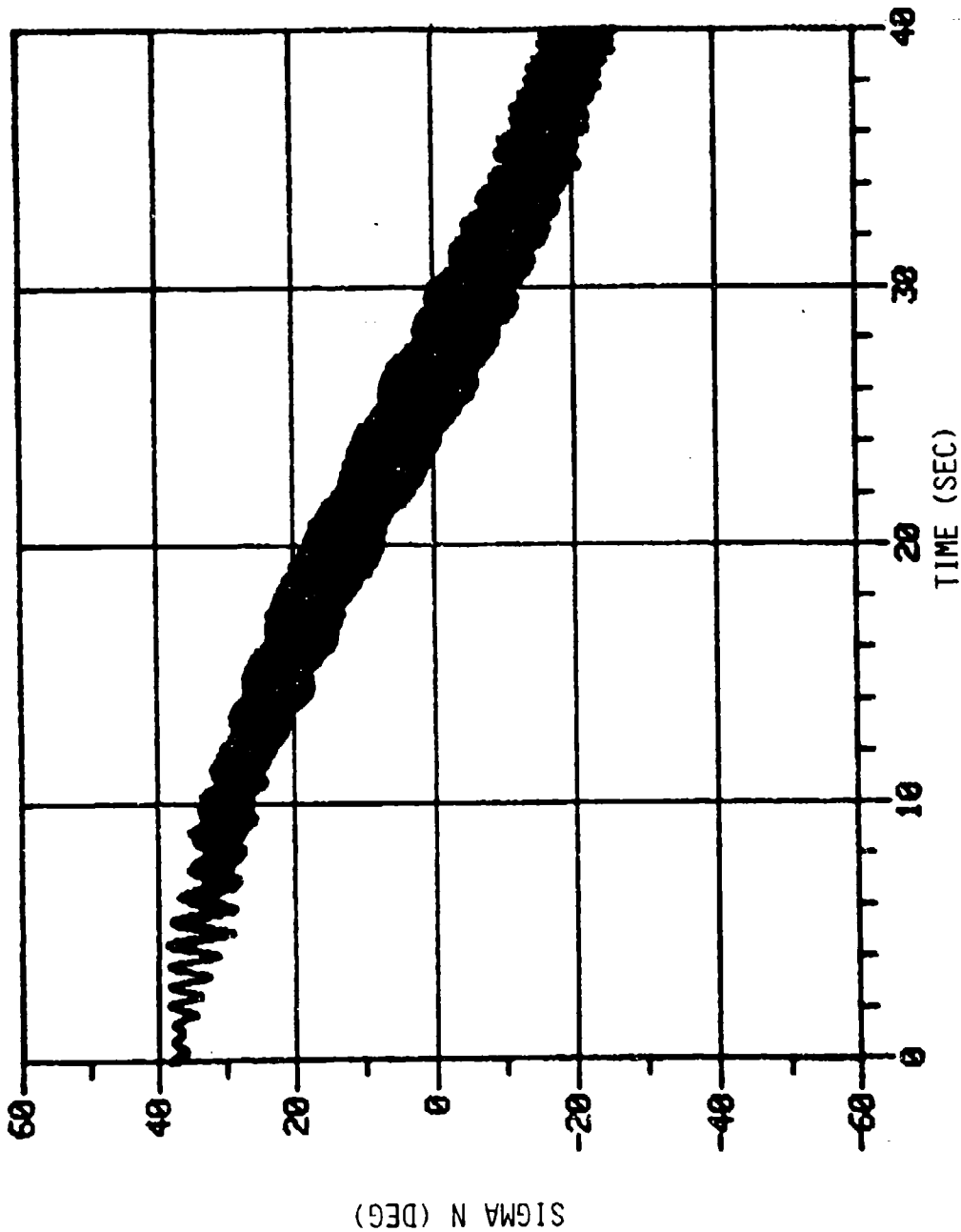


Figure 10a. Sigma N Versus Time for B1-1 (0-40 Sec).

SITE I.D. WALLEOPS BRL ROUND1814 FIRED 09-29-82

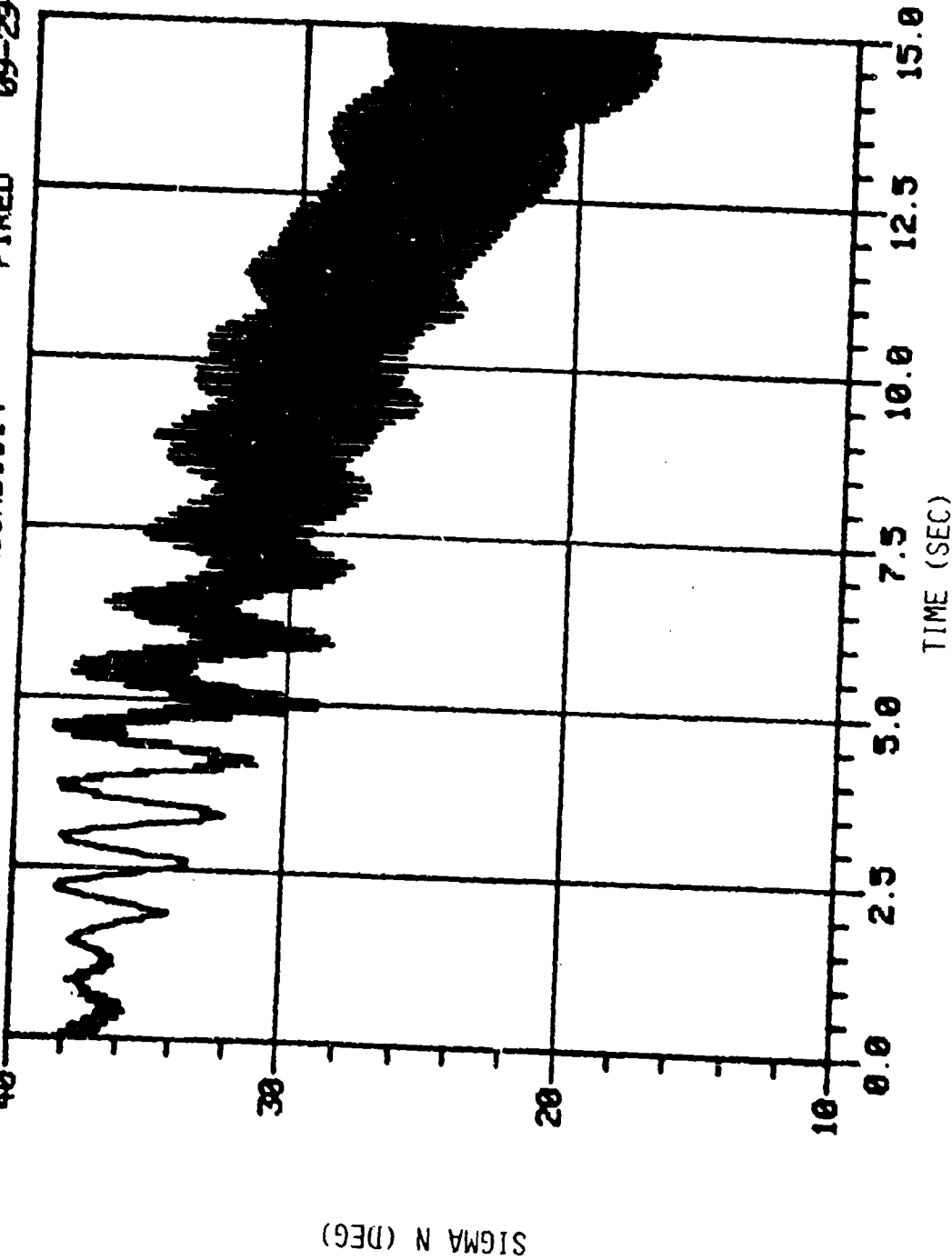


Figure 10b. Sigma N Versus Time for B1-1 (0-15 Sec).

SITE I.O. WALLOPS

BRL ROUND 1814

FIRED

09-23-82

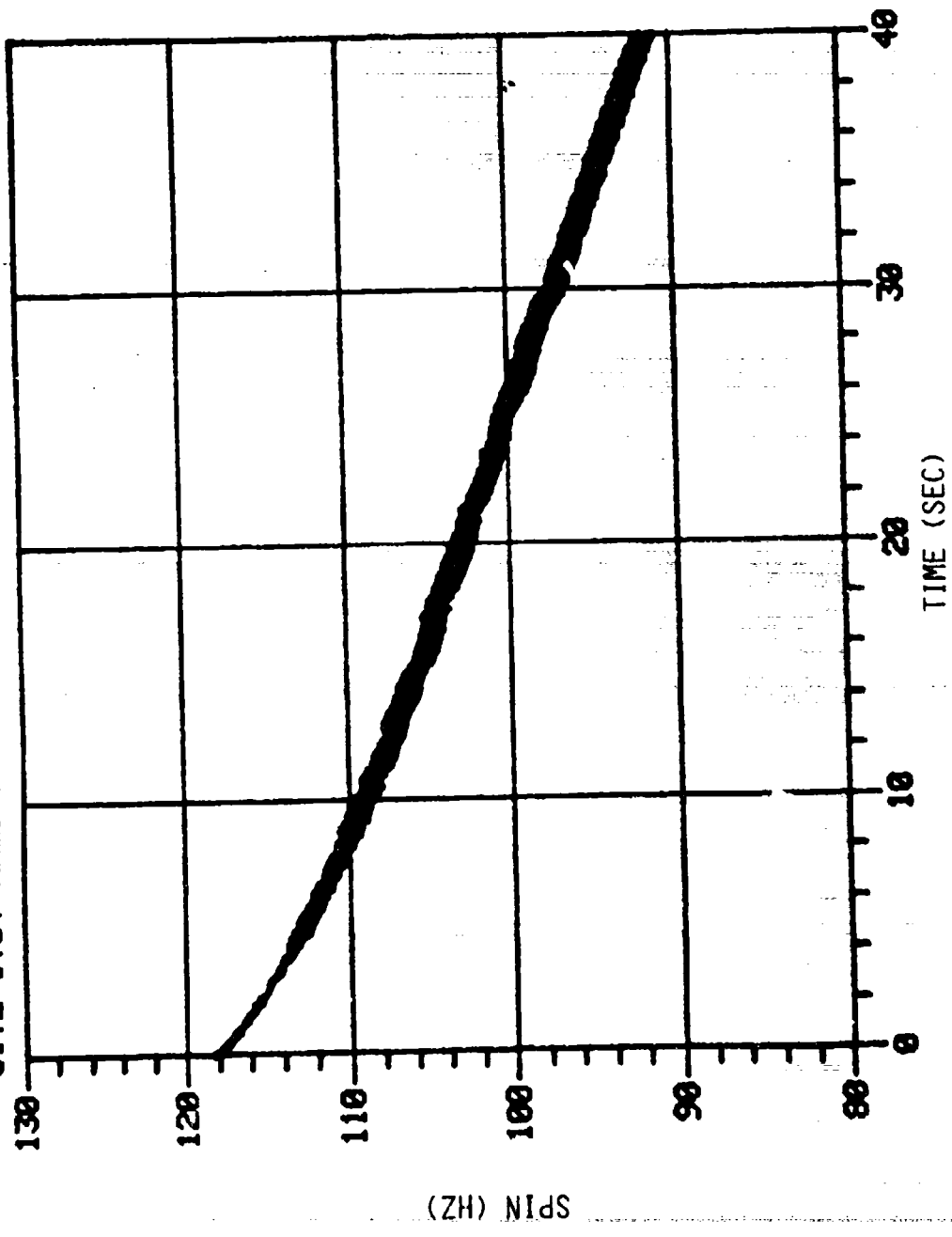


Figure 10c. Spin Versus Time for B1-1.

SITE I.D. WALLEPS

BRL ROUND1815

FIRED

09-29-82

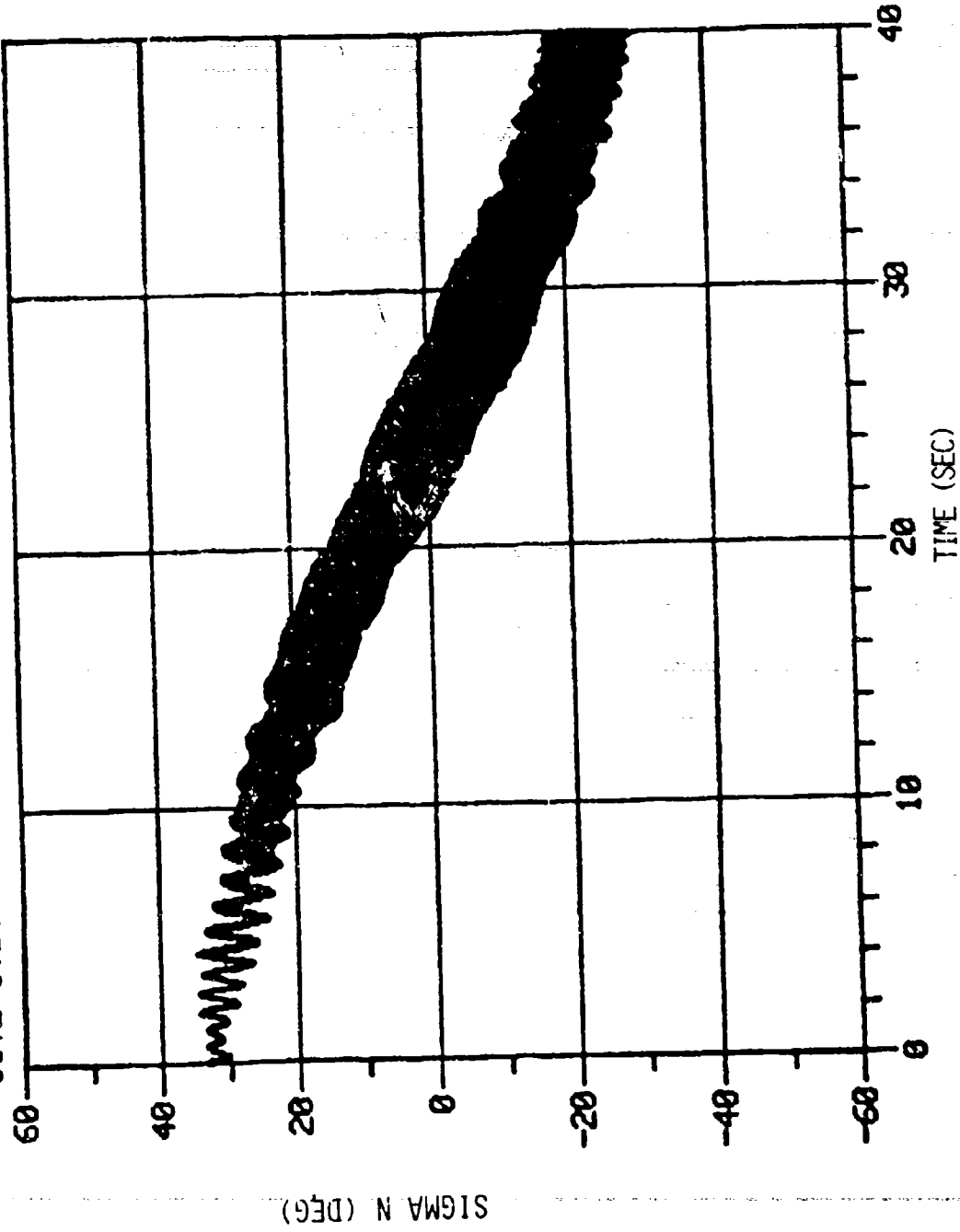


Figure 11a. Sigma N Versus Time for B1-2 (0-40 Sec).

SITE I.O. WALLOPS BRL ROUND1815 FIRED 09-29-82

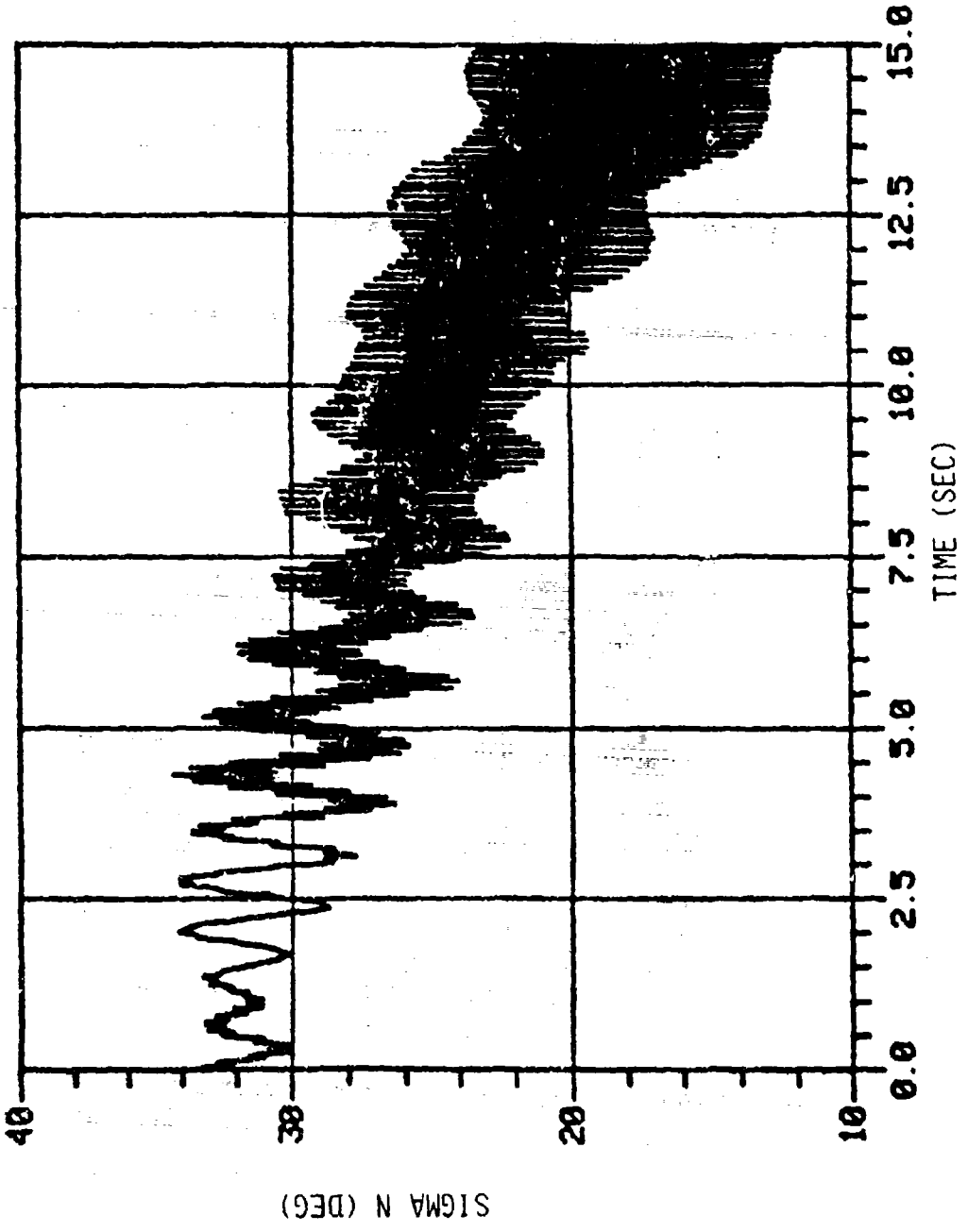


Figure 11b. Sigma N Versus Time for B1-2 (0-15 Sec).

SITE I.D. MALLOPS

BRL ROUND1815

FIRED

03-29-82

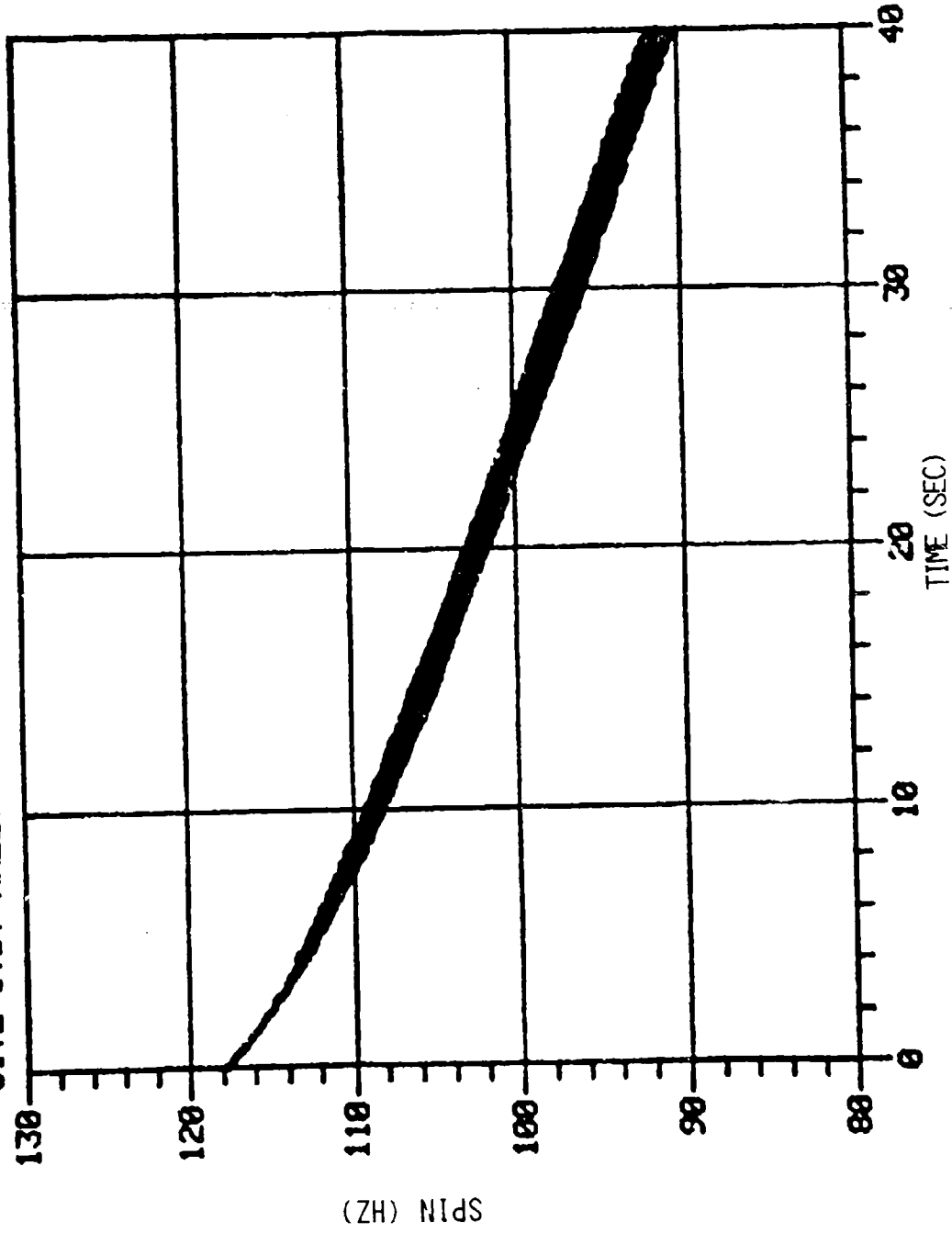


Figure 11c. Spin Versus Time for B1-2.

SITE I.D. WALLEPS BRL ROUND1816 FIRED 09-29-82

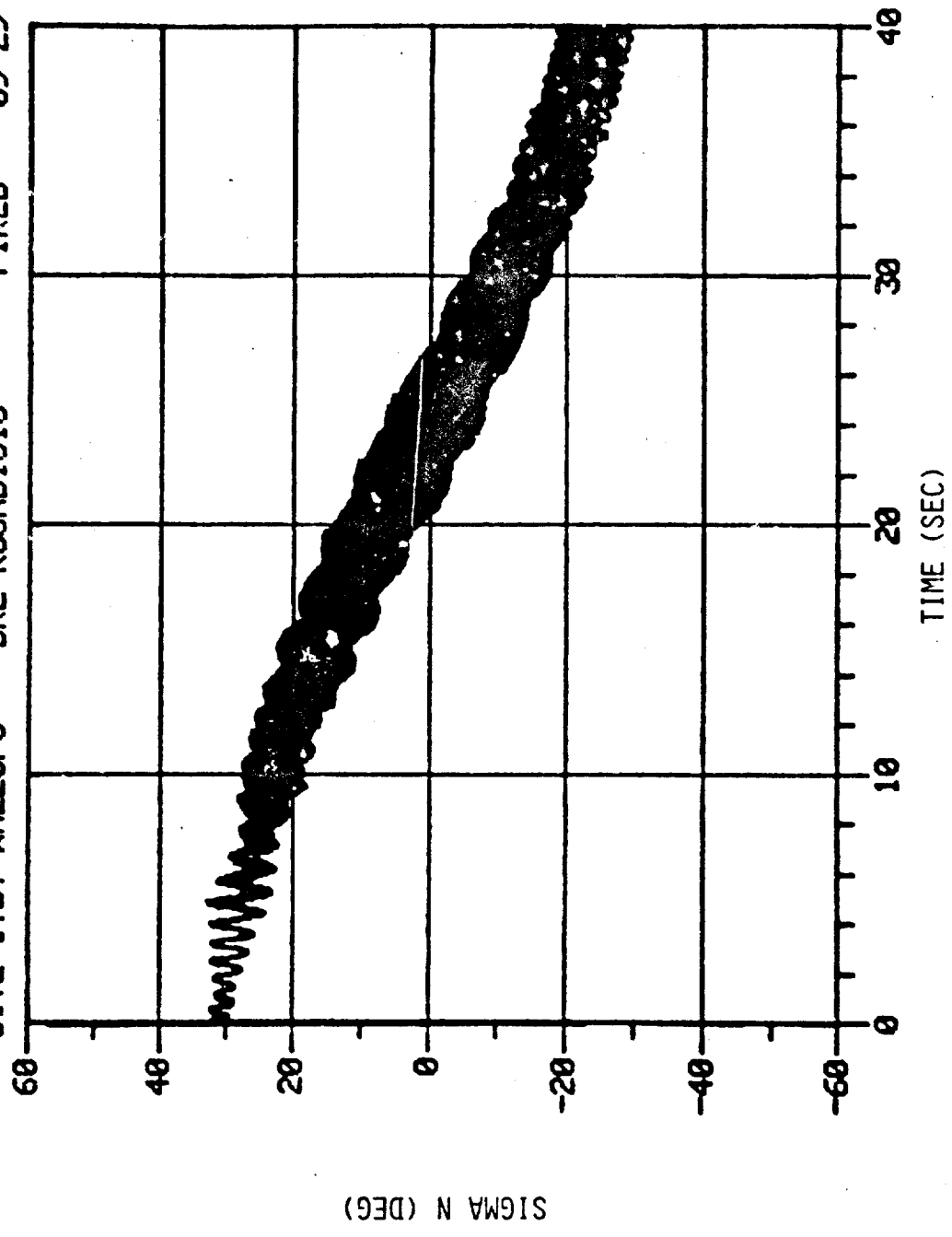


Figure 12a. Sigma N Versus Time for B1-3 (0-40 Sec).

SITE I.D. WALLEPS BRL ROUND1816 FIRED 09-29-82

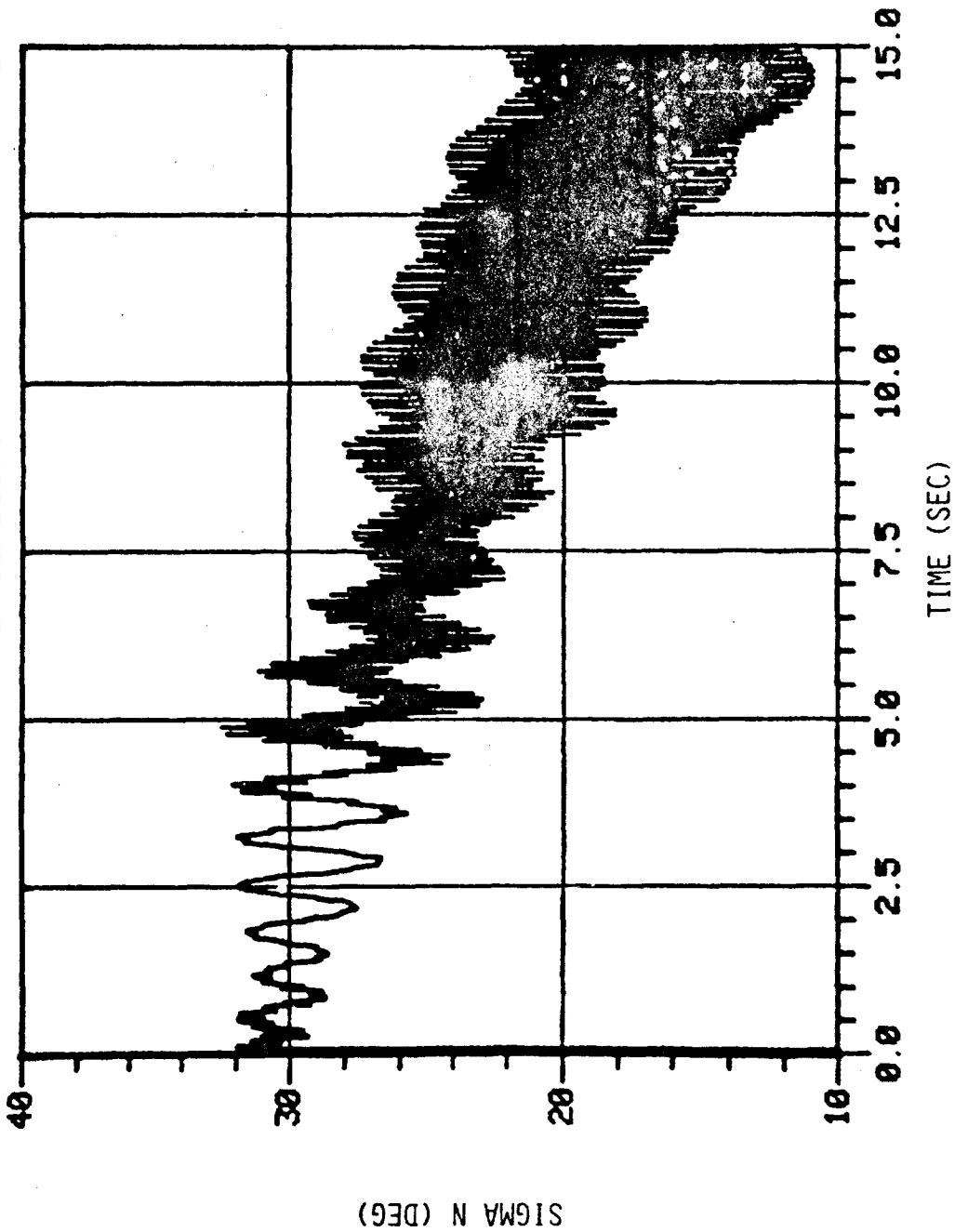


Figure 12b. Sigma N Versus Time for B1-3 (0-15 Sec).

09-29-82

FIRE

BRL ROUND 1816

SITE I. D. WALLEPS

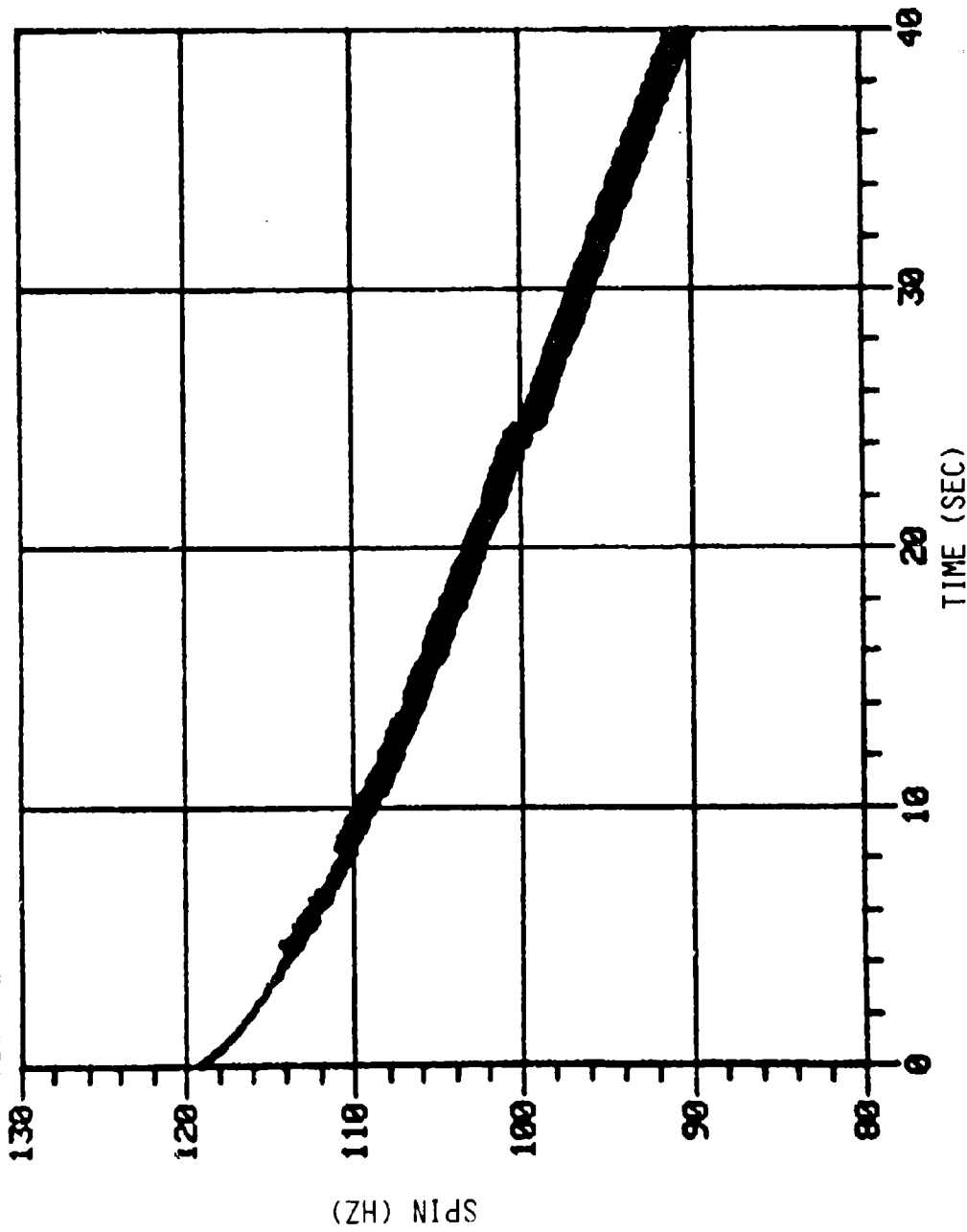


Figure 12c. Spin Versus Time for B1-3.

SITE I.D. WALLOPS BRL ROUND1848 FIRED 09-29-82

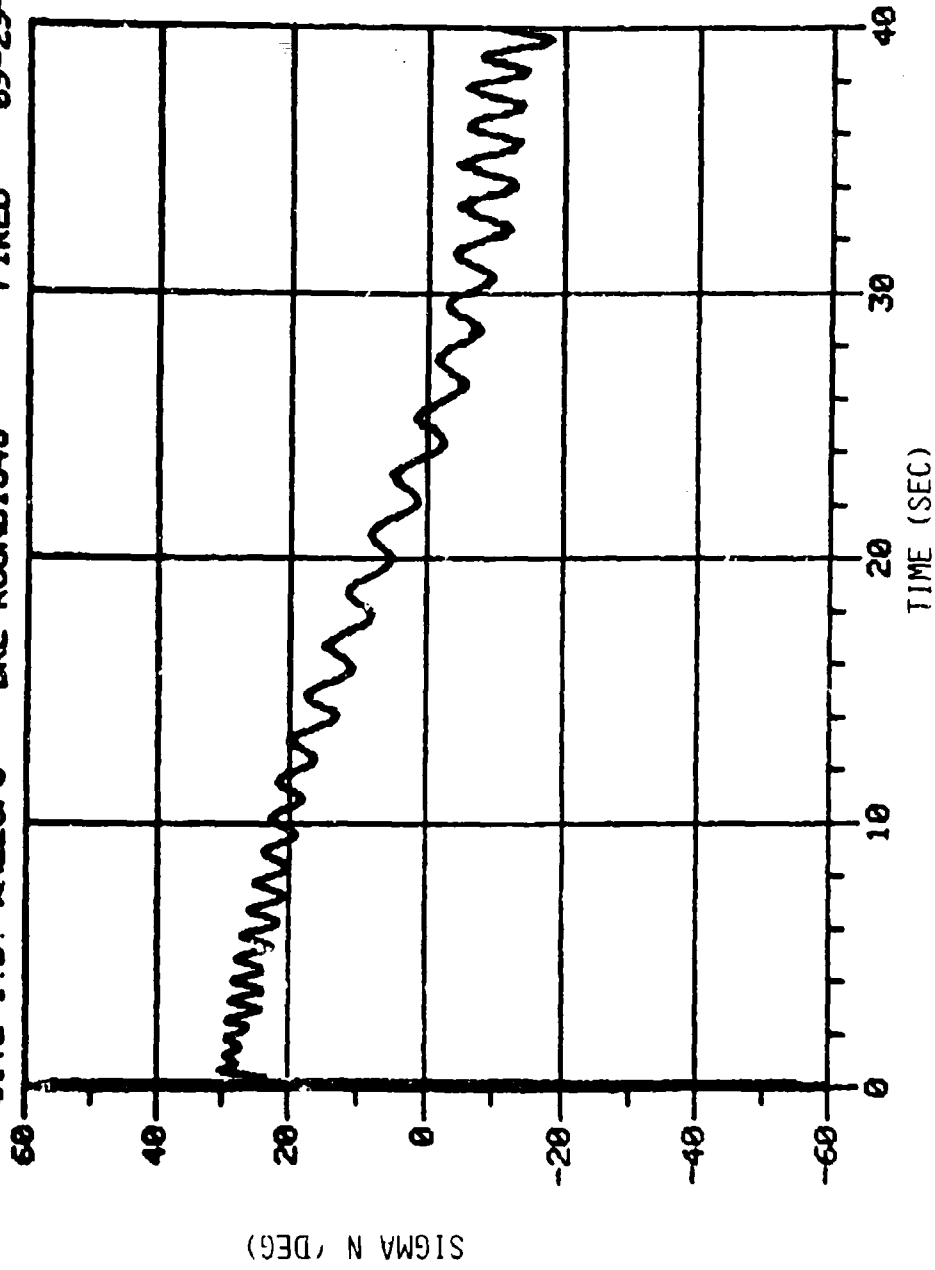


Figure 13a. Sigma N Versus Time for B50-1.

SITE I.O. WALLEOPS BRL ROUND1848 FIRED 09-29-82

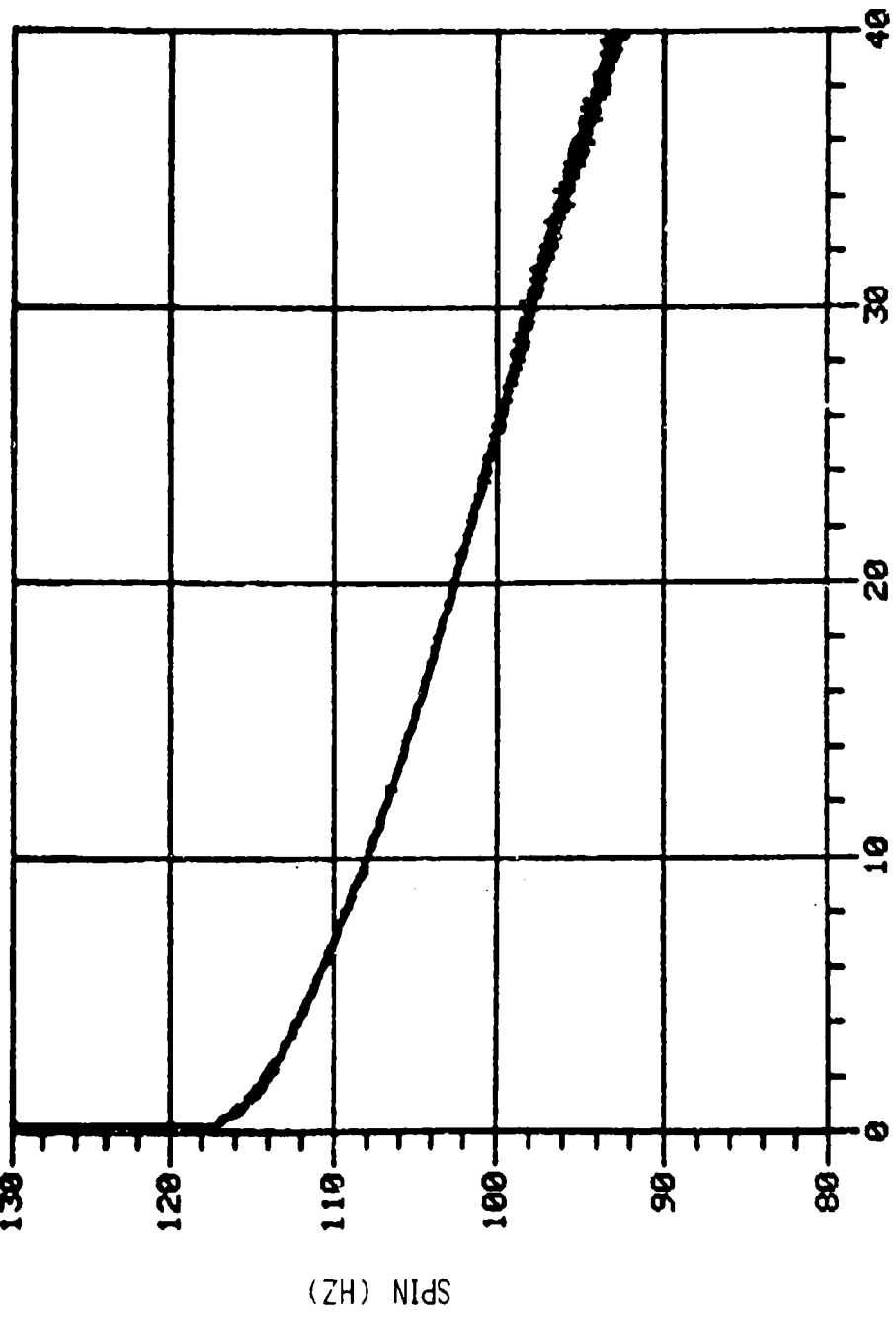


Figure 13b. Spin Versus Time for B50-1.

RE =  $3.98 \times 10^4$ , C/A = 5.20, A SERIES

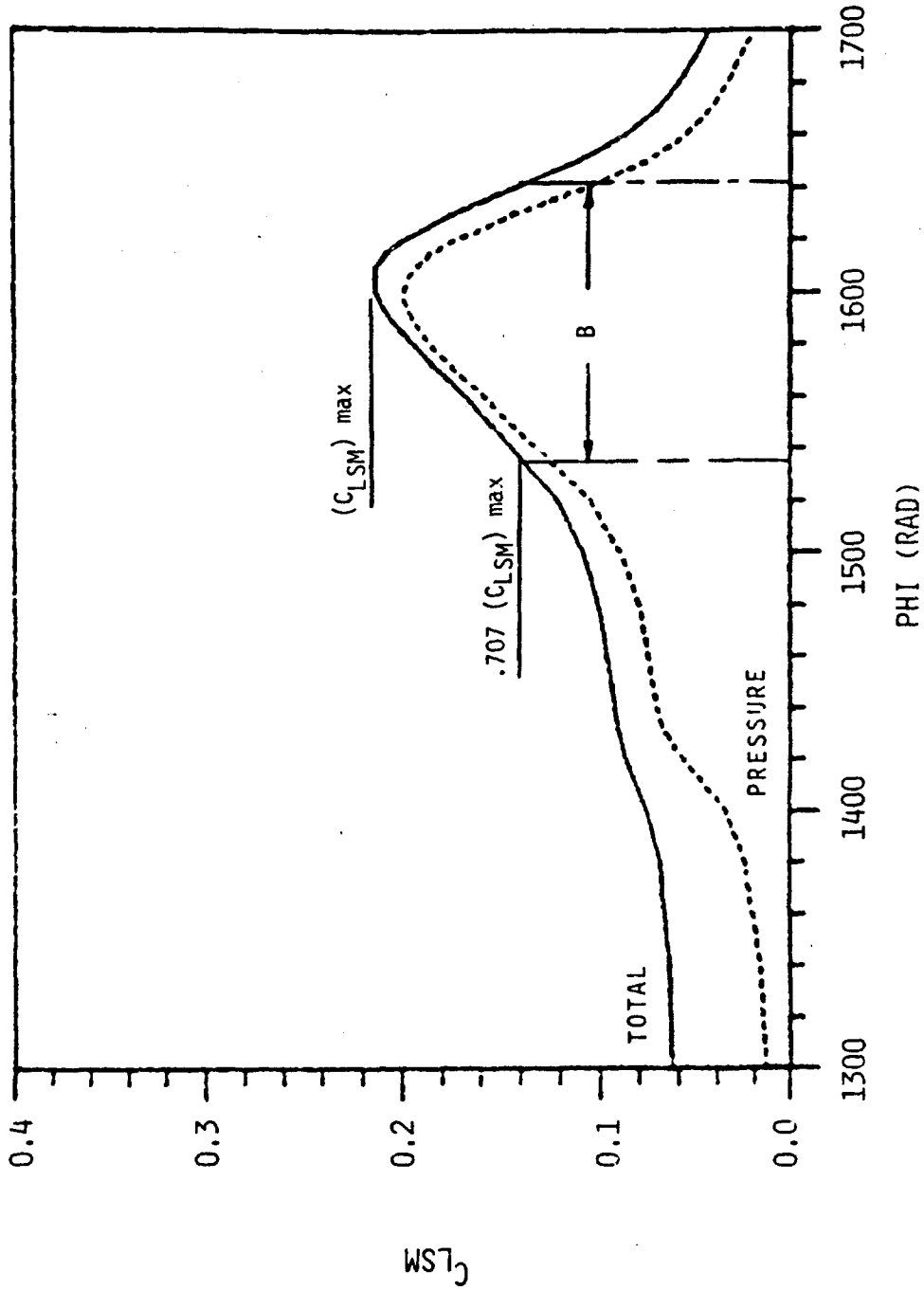


Figure 14a.  $C_{LSM}$  During Spin-Up for  $c/a = 5.20$ .

$C_{LSM}$

RE =  $3.98 \times 10^4$ , C/A = 3.12, B SERIES

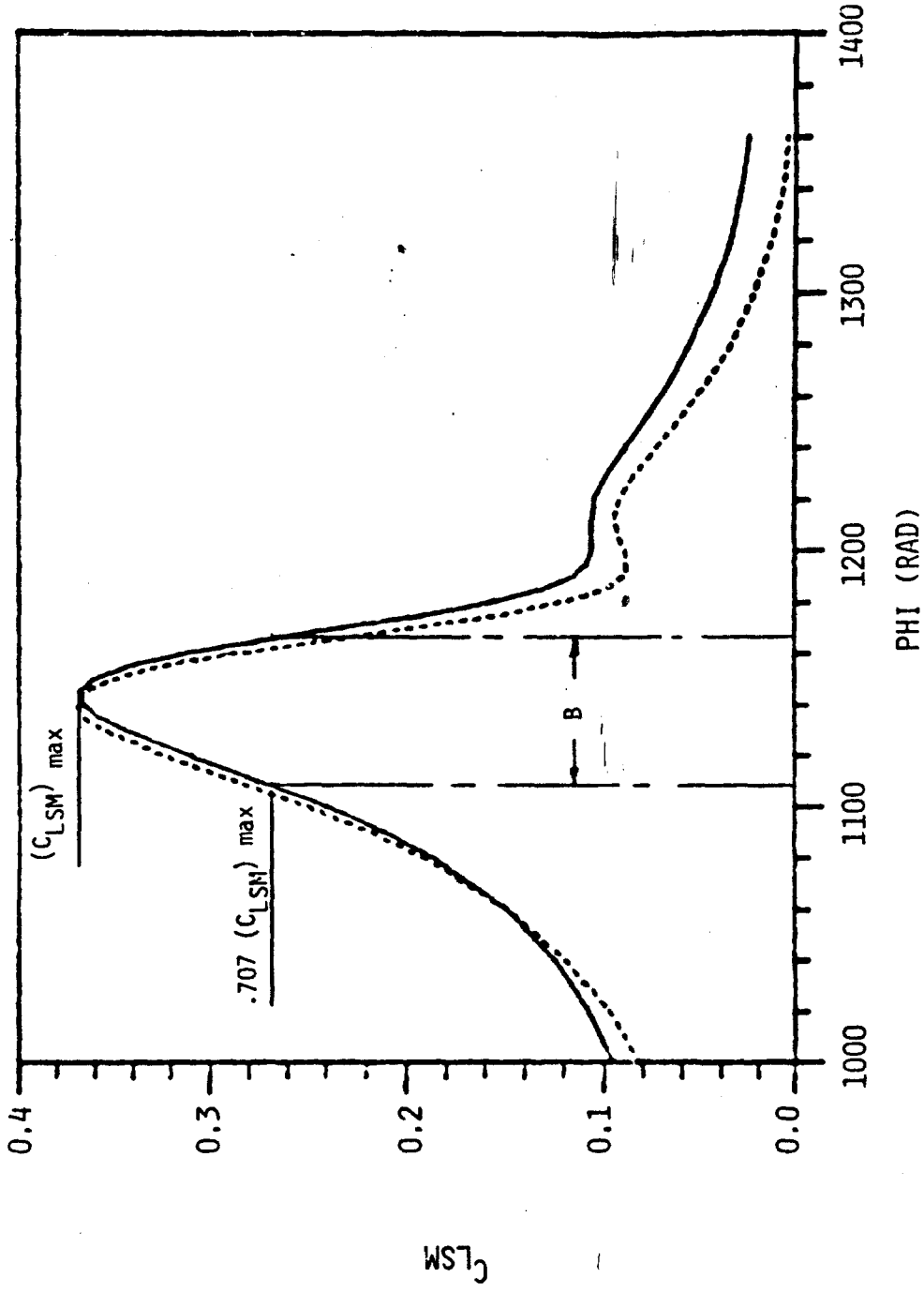


Figure 14b.  $C_{LSM}$  During Spin-Up for  $c/a = 3.12$ .

$C_{LSM}$

## REFERENCES

1. H. P. Greenspan, The Theory of Rotating Fluids, Cambridge University Press, London and New York, 1968.
2. Charles H. Murphy, "Angular Motion of a Spinning Projectile With a Viscous Liquid Payload," BRL Memorandum Report ARBRL-MR-03194, August 1982 (AD A118676). See also Journal of Guidance, Control, and Dynamics, Vol. 6, July-August 1983, pp. 280-286.
3. Nathan Gerber and Raymond Sedney, "Moment on a Liquid-Filled Spinning and Nutating Projectile: Solid Body Rotation," BRL Technical Report ARBRL-TR-02470, February 1983 (AD A125332).
4. E. H. Wedemeyer, "Viscous Corrections to Stewartson's Stability Criterion," BRL Report No. 1325, June 1966 (AD 489687).
5. E. H. Wedemeyer, "The Unsteady Flow Within a Spinning Cylinder," BRL Report No. 1225, October 1963, AD 431846. Also Journal of Fluid Mechanics, Vol. 20, Part 3, 1964, pp. 383-399.
6. C. W. Kitchens, Jr., "Ekman Compatibility Conditions in Wedemeyer Spin-Up Model," The Physics of Fluids, Vol. 23, No. 5, May 1980, pp. 1062-1064.
7. C. W. Kitchens, Jr., "Navier-Stokes Solutions for Spin-Up From Rest in a Cylindrical Container," BRL Technical Report ARBRL-TR-02193, September 1979 (AD A077115).
8. Raymond Sedney and Nathan Gerber, "Viscous Effects in the Wedemeyer Model of Spin-Up From Rest," BRL Technical Report ARBRL-TR-02493, June 1983 (AD A129506).
9. R. Sedney and N. Gerber, "Oscillations of a Liquid in a Rotating Cylinder: Part II. Spin-Up," BRL Technical Report ARBRL-TR-02489, May 1983 (AD A129094).
10. Charles H. Murphy, "Moment Induced by Liquid Payload During Spin-Up Without a Critical Layer," BRL Technical Report in preparation.
11. W. P. D'Amico, W. H. Clay, and A. Mark, "Yawsonde Data for M687-Type Projectiles with Application to Rapid Spin Decay and Stewartson-Type Spin-Up Instabilities," BRL Memorandum Report ARBRL-MR-03027, June 1980 (AD A089646).
12. W. H. Mermagen and W. H. Clay, "The Design of a Second Generation Yawsonde," BRL Memorandum Report ARBRL-MR-2368, April 1974 (AD 780064).

DISTRIBUTION LIST

<u>No. of Copies</u>	<u>Organization</u>	<u>No. of Copies</u>	<u>Organization</u>
12	Administrator Defense Technical Information Center ATTN: DTIC-DDA Cameron Station Alexandria, VA 22314	1	Commander US Army Armament, Munitions and Chemical Command ATTN: DRSMC-LEP-L(R) Rock Island, IL 61299
1	Commander US Army Materiel Development and Readiness Command ATTN: DRCDMD-ST 5001 Eisenhower Avenue Alexandria, VA 22333	1	Director Benet Weapons Laboratory Armament R&D Center US Army AMCCOM ATTN: DRSMC-LCB-TL(D) Watervliet, NY 12189
1	Commander Armament R&D Center US Army AMCCOM ATTN: DRSMC-TDC(D) Dover, NJ 07801	1	Commander US Army Aviation Research and Development Command ATTN: DRDAV-E 4300 Goodfellow Blvd St. Louis, MO 63120
2	Commander Armament R&D Center US Army AMCCOM ATTN: DRSMC-TSS(D) Dover, NJ 07801	1	Director US Army Air Mobility Research and Development Laboratory Ames Research Center Moffett Field, CA 94035
1	Commander Armament R&D Center US Army AMCCOM ATTN: DRSMC-LC(D) Dover, NJ 07801	1	Commander US Army Communications Research and Development Command ATTN: DRSEL-ATDD Fort Monmouth, NJ 07703
1	Commander Armament R&D Center US Army AMCCOM ATTN: DRSMC-CAWS-AM(D) Mr. DellaTerga Dover, NJ 07801	1	Commander US Army Electronics Research and Development Command Technical Support Activity ATTN: DELSD-L Fort Monmouth, NJ 07703
2	Commander Armament R&D Center US Army AMCCOM ATTN: DRSMC-LCA-F(D) Mr. D. Mertz Mr. A. Loeb Dover, NJ 07801	2	Commandant US Army Infantry School ATTN: ATSH-CD-CSO-OR Fort Benning, GA 31905
		1	AFWL/SUL Kirtland AFB, NM 87117

DISTRIBUTION LIST

<u>No. of Copies</u>	<u>Organization</u>	<u>No. of Copies</u>	<u>Organization</u>
1	Commander US Army Missile Command ATTN: DRSMI-R Redstone Arsenal, AL 35898	1	Commander Naval Surface Weapons Center ATTN: Dr. W. Yanta Aerodynamics Branch K-24, Building 402-12 White Oak Laboratory Silver Spring, MD 20910
1	Commander US Army Missile Command ATTN: DRSMI-YDL Redstone Arsenal, AL 35898	1	AFATL (DLDL, Dr. D.C. Daniel) Eglin AFB, FL 32542
1	Commander US Army Missile Command ATTN: DRSMI-RDK, Mr. R. Deep Redstone Arsenal, AL 35898	1	Aerospace Corporation Aero-Engineering Subdivision ATTN: Walter F. Reddall El Segundo, CA 90245
1	Commander US Army Tank Automotive Command ATTN: DRSTA-TSL Warren, MI 48090	2	Director National Aeronautics and Space Administration Ames Research Center ATTN: Dr. P. Kutler Dr. T. Steger Moffett Field, CA 94035
1	Director US Army TRADOC Systems Analysis Activity ATTN: ATAA-SL White Sands Missile Range NM 88002	1	Director National Aeronautics and Space Administration Langley Research Center ATTN: Tech Library Langley Station Hampton, VA 23365
1	Commander US Army Dugway Proving Ground ATTN: STEDP-MT Mr. G. C. Travers Dugway, UT 84022	1	Director National Aeronautics and Space Administration Marshall Space Flight Center ATTN: Dr. W. W. Fowlis Huntsville, AL 35812
1	Commander US Army Yuma Proving Ground ATTN: STEYP-MTW Yuma, AZ 85365	1	Director National Aeronautics and Space Administration Marshall Space Flight Center ATTN: Dr. W. W. Fowlis Huntsville, AL 35812
3	Director Sandia National Laboratory ATTN: Mr. H. R. Vaughn Dr. W. Oberkampf Mr. F. G. Blottner Albuquerque, NM 87115	2	Calspan Corporation ATTN: G. Homicz W. Rae P.O. Box 400 Buffalo, NY 14225

## DISTRIBUTION LIST

<u>No. of Copies</u>	<u>Organization</u>	<u>No. of Copies</u>	<u>Organization</u>
1	Martin-Marietta Corporation ATTN: S.H. Maslen 1450 S. Rolling Road Baltimore, MD 21227	1	University of California - Davis ATTN: H.A. Dwyer Davis, CA 95616
2	Rockwell International Science Center ATTN: Dr. V. Shankar Dr. S. Chakravarthy 1049 Camino Dos Rios Thousand Oaks, CA 91360	1	University of Colorado Department of Astro-Geophysics ATTN: E.R. Benton Boulder, CO 80304
1	Arizona State University Department of Mechanical and Energy Systems Engineering ATTN: G.P. Neitzel Tempe, AZ 85281	2	University of Maryland ATTN: W. Meirik J.D. Anderson College Park, MD 20742
1	Massachusetts Institute of Technology ATTN: H. Greenspan 77 Massachusetts Avenue Cambridge, MA 02139	1	University of Maryland - Baltimore County Department of Mathematics ATTN: Dr. Y.M. Lynn 5401 Wilkens Avenue Baltimore, MD 21228
1	North Carolina State University Mechanical and Aerospace Engineering Department ATTN: F.F. DeJarnette Raleigh, NC 27650	1	University of Santa Clara Department of Physics ATTN: R. Greeley Santa Clara, CA 95053
1	Northwestern University Department of Engineering Science and Applied Mathematics ATTN: Dr. S.H. Davis Evanston, IL 60201	2	University of Southern California Department of Aerospace Engineering ATTN: T. Maxworthy P. Weidman Los Angeles, CA 90007
1	Notre Dame University Department of Aero Engr ATTN: T.J. Mueller South Bend, IN 46556	2	University of Rochester Department of Mechanical and Aerospace Sciences ATTN: R. Gans A. Clark, Jr. Rochester, NY 14627
1	Rensselaer Polytechnic Institute Department of Math Sciences ATTN: R.C. Diprima Troy, NY 12181	1	University of Tennessee Department of Physics ATTN: Prof. W.E. Scott Knoxville, TN 37916

DISTRIBUTION LIST

No. of  
Copies

Organization

- 3 Virginia Polytechnic Institute  
and State University  
Department of Aerospace  
Engineering  
ATTN: Tech Library  
Dr. W. Saric  
Dr. T. Herbert  
Blacksburg, VA 24061
- 1 University of Wyoming  
ATTN: D.L. Boyer  
University Station  
Laramie, WY 82071

Aberdeen Proving Ground

Director, USAMSAA  
ATTN: DRXS-D  
DRXS-MP, Mr. H. Cohen

Commander, USATECOM  
ATTN: DRSTE-TO-F  
DRSTE-CM-F  
Mr. Gibson (2 cys)

PM-SMOKE  
ATTN: DRCPM-SMK-M

Cdr, CRDC, AMCCOM  
ATTN: DRSMC-CLN  
Mr. W. Dee  
Mr. C. Hughes  
Mr. F. Dagostin  
Mr. C. Jeffers  
Mr. L. Shaft  
Mr. M. Parker  
DRSMC-CLB-PA  
Mr. M. C. Miller  
DRSMC-CLJ-IL  
DRSMC-CLJ-L

USER EVALUATION OF REPORT

Please take a few minutes to answer the questions below; tear out this sheet, fold as indicated, staple or tape closed, and place in the mail. Your comments will provide us with information for improving future reports.

1. BRL Report Number \_\_\_\_\_

2. Does this report satisfy a need? (Comment on purpose, related project, or other area of interest for which report will be used.)  
\_\_\_\_\_  
\_\_\_\_\_

3. How, specifically, is the report being used? (Information source, design data or procedure, management procedure, source of ideas, etc.)  
\_\_\_\_\_  
\_\_\_\_\_

4. Has the information in this report led to any quantitative savings as far as man-hours/contract dollars saved, operating costs avoided, efficiencies achieved, etc.? If so, please elaborate.  
\_\_\_\_\_  
\_\_\_\_\_

5. General Comments (Indicate what you think should be changed to make this report and future reports of this type more responsive to your needs, more usable, improve readability, etc.)  
\_\_\_\_\_  
\_\_\_\_\_  
\_\_\_\_\_

6. If you would like to be contacted by the personnel who prepared this report to raise specific questions or discuss the topic, please fill in the following information.

Name: \_\_\_\_\_

Telephone Number: \_\_\_\_\_

Organization Address: \_\_\_\_\_  
\_\_\_\_\_  
\_\_\_\_\_